PRECONDITIONING OF ACTIVE-SET NEWTON METHODS FOR PDE-CONSTRAINED OPTIMAL CONTROL PROBLEMS*

MARGHERITA PORCELLI† , VALERIA SIMONCINI† , AND MATTIA TANI†

Abstract. We address the problem of preconditioning a sequence of saddle point linear systems arising in the solution of PDE-constrained optimal control problems via active-set Newton methods, with control and (regularized) state constraints. We present two new preconditioners based on a full block matrix factorization of the Schur complement of the Jacobian matrices, where the active-set blocks are merged into the constraint blocks. We discuss the robustness of the new preconditioners with respect to the parameters of the continuous and discrete problems. Numerical experiments on 3D problems are presented, including comparisons with existing approaches based on preconditioned conjugate gradients in a nonstandard inner product.

Key words. optimal control problems, Newton's method, active-set, saddle point matrices.

AMS subject classifications. 65F50, 15A09, 65K05.

1. The problem. In this work we consider the family of PDE-constrained optimization problems of the form

$$\min_{\mathrm{y,u}} \frac{1}{2}\|\mathrm{y}-\mathrm{y_d}\|^2_{L^2(\Omega)} + \frac{\nu}{2}\|\mathrm{u}\|^2_{L^2(\Omega)}$$
$$\text{s.t.} \begin{cases} -\Delta \mathrm{y} - \beta\cdot\nabla \mathrm{y} = \mathrm{u} & \text{in } \Omega \\ \mathrm{y} = \bar{\mathrm{y}} & \text{on } \partial\Omega \\ \mathrm{a} \le \alpha_u \mathrm{u} + \alpha_y \mathrm{y} \le \mathrm{b} & \text{a.e. in } \Omega, \end{cases} \tag{1.1}$$

where $\nu \in \mathbb{R}^+$ is a regularization parameter, $\mathrm{y_d}$ is a given function representing the desired state, and Ω is a domain in $\mathbb{R}^d$ with $d = 2, 3$. The state y and the control u are linked via an elliptic convection-diffusion equation with convection direction $\beta \in \mathbb{R}^d$. Dirichlet boundary conditions are assumed. Moreover, we assume the presence of box constraints of the form $\mathrm{a} \le \alpha_\mathrm{u}\mathrm{u} + \alpha_\mathrm{y}\mathrm{y} \le \mathrm{b}$ a.e. in Ω, where we assume $\mathrm{a(x)} < \mathrm{b(x)}$ a.e. in Ω and α_u, α_y nonnegative scalars such that $\max\{\alpha_y, \alpha_u\} > 0$. By varying the parameters α_u, α_y, we obtain optimal control problems with different inequality constraints. In particular, we will consider three specific choices which yield well studied problems. The first is $(\alpha_u, \alpha_y) = (1, 0)$, that is

$$\mathrm{a} \le \mathrm{u} \le \mathrm{b} \quad \text{a.e. in } \Omega, \tag{1.2}$$

which is refereed to as the optimal control problem with *Control Constraints* (CC). The second one is $(\alpha_u, \alpha_y) = (\epsilon, 1)$ yielding an optimal control problem with *Mixed Constraints* (MC) of the form

$$\mathrm{a} \le \epsilon\mathrm{u} + \mathrm{y} \le \mathrm{b} \quad \text{a.e. in } \Omega. \tag{1.3}$$

The third choice is $(\alpha_u, \alpha_y) = (0, 1)$ yielding optimal control problems with *State Constraints* (SC)

$$\mathrm{a} \le \mathrm{y} \le \mathrm{b} \quad \text{a.e. in } \Omega. \tag{1.4}$$

*Version of May 22, 2015. This work was partially supported by *National Group of Computing Science (GNCS-INDAM)*

†Università di Bologna, Dipartimento di Matematica, Piazza di Porta S. Donato 5, 40127 Bologna, Italy. Emails: {margherita.porcelli,valeria.simoncini,mattia.tani2}@unibo.it

Mixed Constraints (1.3) are commonly employed as a form of regularization of the state-constrained problem, where $\epsilon > 0$ represents the regularization parameter [20]. Indeed, pure state constrained problems are more complicated than control constrained ones, as in general the Lagrange multiplier associated with state constraints is only a measure, and therefore regularized versions with better regularity properties are needed to justify the employed solution methods in function space. Examples of typical employed regularizations are the one applied to the state constraints as in (1.3) (see, e.g., [5]) and the one that employs the Moreau-Yosida penalty function [16, 23]. We refer to [20] for a discussion of this point, and for the use of primal-dual active set strategies to deal with the regularized problem. In the following we shall see the purely state-constrained problem as the limit case of the mixed-constrained one. As such, it may provide helpful information as a computational reference for the mixed-constrained problem when ϵ is very small.

We follow a *discretize-then-optimize* approach for the solution of problem (1.1) as we first transform the original continuous problem into a standard Quadratic Programming (QP) problem by a finite difference or finite element discretization, and then we numerically solve the first-order conditions of the fully discretized optimization problem. Issues related to the commutativity between the discretize-then-optimize and the optimize-then-discretize approach for convection diffusion control equations have been addressed in [25].

Due to the presence of inequality constraints in the problem formulation, the optimality system is nonlinear. Moreover, its dimension will be very large as soon as the desired accuracy requires a fine discretization of the partial differential equation; the Lagrange multiplier approach also yields a structured (block) nonlinear equation, thus further expanding the discrete problem size. We therefore apply a Newton-type approach for the nonlinear equation solution, and we use a Krylov subspace method to solve the arising sequence of large and sparse saddle point linear systems. It is well-known that a computationally effective solution of the linear algebra phase is crucial for the practical implementation of the Newton-Krylov method [7] and it is widely recognized that preconditioning is a critical ingredient of the iterative solver.

Existing preconditioners for constrained optimal control problems have been tailored for specific elements of the family (1.1) and are generally suitable for problems where the operator characterizing the PDE is self-adjoint. Moreover, implementations based on the preconditioned conjugate gradient method in a nonstandard inner product have often been preferred, in spite of possible strong limitations [14, 23, 34]. The works [23, 34] are for CC problems governed by symmetric PDEs, while [14] considers problems with constraints (1.2)-(1.4) but mostly focuses on $\beta = 0$. In particular, the problematic numerical behavior of the preconditioners proposed in [14] for $\beta \neq 0$ motivated this work.

In this paper, we present two new preconditioners aimed at enhancing the solution of the linear algebra phase arising from the discretization of the family of optimal control problems involving state and/or control constraints of the form (1.1). We consider an indefinite preconditioner and a symmetric and positive definite block diagonal preconditioner. Both strategies rely on a general factorized approximation of the Schur complement, and embed newly formed information of the nonlinear iteration, so that they dynamically change as the nonlinear iteration proceeds. The proposed preconditioners are very versatile, as they allow to handle mixed constraints as well as the corresponding limit cases, that is control and state constraints. In particular, we derive optimality and robustness theoretical properties for the spectrum

of the preconditioned matrices, which hold for a relevant class of problem parameters; numerical experiments support this optimality also in terms of CPU time. A broad range of numerical experiments on three test problems is reported, for a large selection of the four problem parameters (ν, β, ϵ and the spatial mesh size h), indicating only a mild sensitivity of the preconditioner with respect to these values, especially when compared with existing approaches (for the parameters for which these latter strategies are defined). In addition, in most cases the indefinite preconditioner outperforms by at least 50% the block diagonal preconditioner, for the same Schur complement approximation.

The outline of the paper is as follows. Sections 2.1 and 2.2 describe the discrete problem and its formal numerical solution by an active-set Newton method. Section 3 reviews the preconditioning strategies that have been devised to solve (1.1) for some choices of the selected parameters. In Section 4 a new general approximation to the Schur complement is introduced and theoretically analyzed, while its impact on the new global preconditioners is investigated in Section 5. Section 6 is devoted to a wide range of numerical results. In particular, in Section 6.1 we discuss some algorithmic details, while in Section 6.2 we report on our numerical experiments on three model problems. Section 7 summarizes our conclusions.

The following notation will be used throughout the paper. For a given square matrix A, spec(A) denotes the set of its eigenvalues. The Euclidean norm for vectors and the induced norm for matrices is used; x^T denotes the transpose of the vector x.

2. Description of the problem.

2.1. The discrete optimization problem. Let M represent the lumped mass matrices in an appropriate finite element space, and L be the discretization of the differential operator $\mathcal{L}(\mathrm{y}) = -\Delta \mathrm{y} + \beta \cdot \nabla \mathrm{y}$; in particular, L is a nonsymmetric matrix of the form $L = K + C$, where K is the symmetric and positive definite discretization of the (negative) Laplacian operator and C is the "convection" matrix. In the following we shall assume that $L + L^T \succeq 0$ [1] Moreover, let n_h be the dimension of the discretized space depending on the mesh size h and let $y, u, a, b \in \mathbb{R}^{n_h}$ be the coefficients of $\mathrm{y}, \mathrm{u}, \mathrm{a}, \mathrm{b}$ in the chosen finite element space basis. Then, the discretization of problem (1.1) is given by the following QP problem

$$\begin{aligned} &\min_{y,u} Q(u,y) = \frac{1}{2}(y - y_d)^T M (y - y_d) + \frac{\nu}{2} u^T M u \\ &\text{s.t.} \quad \begin{cases} Ly = Mu - d \\ a \le \alpha_u u + \alpha_y y \le b \end{cases} \end{aligned} \tag{2.1}$$

where d represents the boundary data. The Lagrangian function for problem (2.1) is given by

$$\mathcal{L}(u, y, p, \mu) = Q(u, y) + (Ly - Mu + d)^T p + (\alpha_u u + \alpha_y y - b)^T \mu_b + (\alpha_u u + \alpha_y y - a)^T \mu_a$$

where p is the Lagrange multiplier associated with the linear equality constraint and μ_a, μ_b are the Lagrange multipliers associated with the lower and upper bound con-

[1] This requirement is satisfied when, for instance, upwind finite differences over a regular grid, or upwind-type finite elements are used, with Dirichlet boundary conditions; see, e.g., [11, Chapter 3], [13].

straints. The corresponding Karush-Kuhn-Tucker conditions are

$$\begin{array}{l} \nabla_y \mathcal{L} = M(y - y_d) + L^T p + \alpha_y(\mu_b + \mu_a) = 0 \\ \nabla_u \mathcal{L} = \nu M u - M p + \alpha_u(\mu_b + \mu_a) = 0 \\ Ly - Mu + d = 0 \\ \mu_b \geq 0, \quad \alpha_u u + \alpha_y y \leq b, \quad \mu_b^T(\alpha_u u + \alpha_y y - b) = 0 \\ \mu_a \leq 0, \quad a \leq \alpha_u u + \alpha_y y, \quad \mu_a^T(a - \alpha_u u - \alpha_y y) = 0 \end{array} \tag{2.2}$$

Setting $\mu = (\mu_b + \mu_a)$, the complementarity conditions in (2.2) can be equivalently stated as the following nonlinear system

$$C(u, y, \mu) = 0$$

with C the following complementary function

$$C(u, y, \mu) = \mu - \max\{0, \mu + c(\alpha_u u + \alpha_y y - b)\} - \min\{0, \mu + c(\alpha_u u + \alpha_y y - a)\}, \tag{2.3}$$

with $c > 0$. Therefore, the KKT system (2.2) can be reformulated as the following nonlinear system

$$F(y, u, p, \mu) = \begin{bmatrix} M(y - y_d) + L^T p + \alpha_y \mu \\ \nu M u - M p + \alpha_u \mu \\ Ly - Mu + d \\ C(u, y, \mu) \end{bmatrix} = 0 \tag{2.4}$$

with $F : \mathbb{R}^{4n_h} \to \mathbb{R}^{4n_h}$, $y, u, p, \mu \in \mathbb{R}^{n_h}$.

2.2. The active-set Newton method. In the following we recall a possible derivation of an active-set Newton type method for the solution of the KKT nonlinear system (2.4) following the description made in [15] where nonsmooth analysis was used.

Let us define the sets of active and inactive indices at the (discrete) optimal solution (u^*, y^*)

$$\mathcal{A}_* = \mathcal{A}_*^b \cup \mathcal{A}_*^a \quad \text{and} \quad \mathcal{I}_* = \{1, \ldots, n_h\} \setminus \mathcal{A}_*, \tag{2.5}$$

where $\mathcal{A}_*^b, \mathcal{A}_*^a$ are the set

$$\mathcal{A}_*^b = \{i \mid \mu_i^* + c(\alpha_u u_i^* + \alpha_y y_i^* - b_i) > 0\}, \quad \mathcal{A}_*^a = \{i \mid \mu_i^* + c(\alpha_u u_i^* + \alpha_y y_i^* - a_i) < 0\}.$$

The nonlinearity and nonsmoothness of the function F in (2.4) are clearly gathered in the last block containing the complementarity function $C(u, y, \mu)$ defined in (2.3). Hintermüller et al. showed in [15] that the functions $v \to \min\{0, v\}$ and $v \to \max\{0, v\}$ from $\mathbb{R}^n \to \mathbb{R}^n$ are slantly differentiable with slanting functions given by the diagonal matrices $G_{\min}(v)$ and $G_{\max}(v)$ with diagonal elements

$$G_{\min}(v)_{ii} = \begin{cases} 1 & \text{if } v_i < 0 \\ 0 & \text{else} \end{cases}, \quad G_{\max}(v)_{ii} = \begin{cases} 1 & \text{if } v_i > 0 \\ 0 & \text{else} \end{cases}$$

The choice of $G_{\min}$ and $G_{\max}$ suggests to use the following element $F'(y^*, u^*, p^*, \mu^*) \in \mathbb{R}^{4n_h \times 4n_h}$ of the generalized Jacobian $\partial F(y^*, u^*, p^*, \mu^*)$ ([6])

$$F'(y^*, u^*, p^*, \mu^*) = \begin{bmatrix} M & 0 & L^T & \alpha_y I \\ 0 & \nu M & -M & \alpha_u I \\ L & -M & 0 & 0 \\ c\alpha_y \Pi_{\mathcal{A}_*} & c\alpha_u \Pi_{\mathcal{A}_*} & 0 & \Pi_{\mathcal{I}_*} \end{bmatrix}, \tag{2.6}$$

to construct a "semismooth" Newton scheme. Here $\Pi_{\mathcal{C}}$ denotes a diagonal binary matrix with nonzero entries in $\mathcal{C}$, and the sets $\mathcal{A}_*, \mathcal{I}_*$ are given in (2.5).

Given the kth iterate (y_k, u_k, p_k, μ_k), let $\mathcal{A}_k$ and $\mathcal{I}_k$ be the current active and inactive sets where

$$\mathcal{A}_k = \mathcal{A}_k^b \cup \mathcal{A}_k^a, \quad \mathcal{I}_k = \{1, \dots, n_h\} \setminus \mathcal{A}_k \tag{2.7a}$$

$$\mathcal{A}_k^b = \{i \mid (\mu_k)_i + c(\alpha_u(u_k)_i + \alpha_y(y_k)_i - b_i) > 0\} \tag{2.7b}$$

$$\mathcal{A}_k^a = \{i \mid (\mu_k)_i + c(\alpha_u(u_k)_i + \alpha_y(y_k)_i - a_i) < 0\} \tag{2.7c}$$

and let $n_{\mathcal{A}_k} = card(\mathcal{A}_k)$ be the current number of active constraints. Using the Jacobian F' in (2.6), the semismooth Newton iteration [15] applied to system (2.4) is the following:

$$\begin{bmatrix} M & 0 & L^T & \alpha_y I \\ 0 & \nu M & -M & \alpha_u I \\ L & -M & 0 & 0 \\ c\alpha_y \Pi_{\mathcal{A}_k} & c\alpha_u \Pi_{\mathcal{A}_k} & 0 & \Pi_{\mathcal{I}_k} \end{bmatrix} \begin{bmatrix} y_{k+1} \\ u_{k+1} \\ p_{k+1} \\ \mu_{k+1} \end{bmatrix} = \begin{bmatrix} My_d \\ 0 \\ d \\ c(\Pi_{\mathcal{A}_k^b} b + \Pi_{\mathcal{A}_k^a} a) \end{bmatrix}.$$

Setting $(\mu_{k+1})_{\mathcal{I}_k} = 0$ (the multiplier associated with the inactive inequality constraints) and eliminating this variable, we obtain the sequence of Newton structured equations

$$J_k x_{k+1} = f_k, \quad k = 1, 2, \dots \tag{2.8}$$

where $x_{k+1} = (y_{k+1}, u_{k+1}, p_{k+1}, (\mu_{k+1})_{\mathcal{A}_k}) \in \mathbb{R}^{3n_h + n_{\mathcal{A}_k}}$,

$$f_k = \begin{bmatrix} My_d \\ 0 \\ d \\ P_{\mathcal{A}_k^b} b + P_{\mathcal{A}_k^a} a \end{bmatrix}, \quad J_k = \begin{bmatrix} M & 0 & L^T & \alpha_y P_{\mathcal{A}_k}^T \\ 0 & \nu M & -M & \alpha_u P_{\mathcal{A}_k}^T \\ L & -M & 0 & 0 \\ \alpha_y P_{\mathcal{A}_k} & \alpha_u P_{\mathcal{A}_k} & 0 & 0 \end{bmatrix}, \tag{2.9}$$

where $P_{\mathcal{C}}$ is a rectangular matrix consisting of those rows of $\Pi_{\mathcal{C}}$ which belong to the indices in $\mathcal{C}$; with this notation, $\Pi_{\mathcal{C}} = P_{\mathcal{C}}^T P_{\mathcal{C}}$. We remark that the value of c has no influence on the solution of the Newton equation (2.8) but affects the updating of the active sets $\mathcal{A}_k$ in (2.7).

The above semismooth Newton scheme was proved to be equivalent to the Primal-Dual active-set method for solving constrained optimal control problems in [15] and this equivalence allowed to establish superlinear local and also global convergence results [15, 20, 18]. In fact, the active-set strategy works as a prediction technique in the sense that it is proved that if $(u_k, y_k, p_k, \mu_k) \to (u^*, y^*, p^*, \mu^*)$, then there exists an index $\bar{k}$ such that $\mathcal{A}_{\bar{k}} = \mathcal{A}_*$ and $\mathcal{I}_{\bar{k}} = \mathcal{I}_*$ [15, Remark 3.4].

Given x_k, the next iterate x_{k+1} is commonly computed by applying an iterative solver (in our case a preconditioned Krylov subspace method) to the Newton equation (2.8), and then generating a sequence of (inner) iterations $\{x_{k+1}^j\}_{j \geq 0}$. The inner iteration is started with $x_{k+1}^0 = x_k$ and stopped for $j_* > 0$ such that

$$\|J_k x_{k+1}^{j_*} - f_k\| \leq \eta_k \|J_k x_{k+1}^0 - f_k\| \tag{2.10}$$

and the next iterate x_{k+1} is set equal to $x_{k+1}^{j_*}$. The scalar $\eta_k > 0$ controls the accuracy in the solution of the unpreconditioned linear system. The choice $\eta_k = \eta_k^E$ with

$$\eta_k^E = \tau_1, \tag{2.11}$$

$k \geq 1$, with a small τ_1 (e.g. $\tau_1 = 10^{-10}$) allows us to compare various preconditioning techniques in solving the linear system (2.8), while the nonlinear iteration remains substantially unaffected by the use of each different inner strategy. This stopping criterion was used in all our numerical experiments of Sections 6.2.1 and 6.2.2.

Occasionally, for some choice of problem parameters we have experienced slow convergence of the Newton method in the solution of CC problems. This prompted us to also consider the adaptive choice $\eta_k = \eta_k^I$

$$\eta_0^I = \tau_2, \quad \eta_k^I = \min\{\eta_{k-1}^I, \tau_3 \|F(u_k, y_k, p_k, \mu_k)\|^2\}, \tag{2.12}$$

$k \geq 1$ (e.g. with $\tau_2 = 10^{-4}, \tau_3 = 10^{-2}$), which gives rise to the "inexact" solution of the Newton system [9, 17, 27]. In particular, (2.12) is intended to give the desirably fast local convergence near a solution and, at the same time, to minimize the occurrence of problem oversolving. We remark that the global convergence of the active set Newton method is no longer guaranteed if inexact steps are computed, but it is anyway expected for small values of the initial forcing term η_0^I [17]. Numerical tests with (2.12) are reported in Section 6.2.3.

The key step in the overall process is the efficient iterative solution of the linear systems (2.8), for which preconditioning is mandatory. The rest of the paper is thus devoted to the analysis of effective preconditioning strategies.

3. Overview of the current approaches. In this section we review some of the preconditioning strategies that have been explored in the literature for the solution of CC, MC and SC problems. In particular we consider the proposals [14, 34] both based on the use of the Preconditioned Conjugate Gradient method [4, 30] with a nonstandard inner product for the solution of the saddle point linear systems arising in the active-set Newton method for solving (2.4). This approach (from now on named BPCG) was originally used in the context of saddle point linear systems for mixed approximations of elliptic problems by Bramble and Pasciak in [4], and then subsequently used in different settings where similar linear systems arise; see, e.g., [14, 30] in our context. Herzog and Sachs in [14] consider the solution of CC, MC and SC problems by partitioning the Jacobian matrix J_k as follows

$$J_k = \left[\begin{array}{cc|cc} M & 0 & L^T & \alpha_y P_{\mathcal{A}_k}^T \\ 0 & \nu M & -M & \alpha_u P_{\mathcal{A}_k}^T \\ \hline L & -M & 0 & 0 \\ \alpha_y P_{\mathcal{A}_k} & \alpha_u P_{\mathcal{A}_k} & 0 & 0 \end{array}\right] = \begin{bmatrix} A & B_k^T \\ B_k & 0 \end{bmatrix}, \tag{3.1}$$

and therefore considering $(\alpha_y, \alpha_u) = (0, 1)$ in the CC case, $(\alpha_y, \alpha_u) = (1, \epsilon)$ in the MC case and $(\alpha_y, \alpha_u) = (1, 0)$ in the SC case. Following the approach presented in [30], Herzog and Sachs proposed the preconditioner

$$\mathcal{P}_k^{\sigma,\tau} = \begin{bmatrix} I & 0 \\ B_k \widehat{A}(\sigma)^{-1} & I \end{bmatrix} \begin{bmatrix} \widehat{A}(\sigma) & B_k^T \\ 0 & -\widehat{S}_k(\sigma, \tau) \end{bmatrix}, \tag{3.2}$$

where $\widehat{A}(\sigma)$ and $\widehat{S}_k(\sigma, \tau)$ approximate the $(1,1)$ block A and the Schur complement S_k respectively, and are block diagonal matrices, while the scalars σ and τ are suitably chosen positive scalars, whose role will be made clear below. A feature of this approach is that the blocks of $\widehat{A}(\sigma)$ and $\widehat{S}_k(\sigma, \tau)$ can be chosen as (approximations of) the inner product matrices of the spaces where the continuous unknowns (y, u) and (p, μ) are

sought. In particular,

$$\widehat{A}(\sigma) = \frac{1}{\sigma}\begin{bmatrix} K & 0 \\ 0 & M \end{bmatrix} \quad \text{and} \quad \widehat{S}_k(\sigma,\tau) = \frac{\sigma}{\tau}\begin{bmatrix} K & 0 \\ 0 & P_{\mathcal{A}_k} M^{-1} P_{\mathcal{A}_k}^T \end{bmatrix},$$

where K is associated with the scalar product in the discretized state space, and the scaling parameters σ and τ are associated with the bilinear forms underlying the considered problems (note that $K = L$ if $\beta = 0$).

The role of the scalars σ and τ is crucial since they have to ensure that $\widehat{A}(\sigma) > A$ and $B_k \widehat{A}(\sigma)^{-1} B_k^T > \widehat{S}_k(\sigma,\tau)$, so that the preconditioned matrix $(\mathcal{P}_k^{\sigma,\tau})^{-1} J_k$ is positive definite with respect to the inner product defined by

$$\mathcal{D}_k^{\sigma,\tau} = \mathcal{P}_k^{\sigma,\tau} - J_k = \begin{bmatrix} \widehat{A}(\sigma) - A & 0 \\ 0 & B_k \widehat{A}(\sigma)^{-1} B_k^T - \widehat{S}_k(\sigma,\tau) \end{bmatrix}.$$

Under these conditions, the CG method in this non-Euclidean inner product can be used.

The spectral analysis provided in [14, Corollary 2.3] for L symmetric ($\beta = 0$) shows that the eigenvalues of $(\mathcal{P}_k^{\sigma,\tau})^{-1} J_k$ are bounded independently of h, while they depend on ν in such a way that the condition number of the preconditioned matrix is proportional to $1/\nu$; As a consequence, poor convergence of BPCG for small values of ν is predicted, and also verified experimentally. Moreover, the authors show that the (preconditioned) condition number in MC problems scales like ϵ^{-2} for small ϵ, making the use of the proposed preconditioner prohibitive for values of ϵ smaller than 10^{-3}. Regarding the analysis for problems with $\beta = (\beta_1, 0, 0)$, $\beta_1 > 0$, a deterioration of the convergence behavior for large values of β_1 was theoretically analyzed for CC problems and confirmed in the few reported experiments. The difficulties in solving these problems are illustrated in the plots of Figure 3.1 which are in complete agreement with [14, Figure 4], and were obtained with the same codes[2], though on a different machine. In particular, we emphasize the strong dependence on β and h of the preconditioned strategy.

In [34] CC problems with a self-adjoint and positive definite elliptic operator as constraint is considered. Differently from [14], at each nonlinear iteration a saddle point system is obtained by eliminating $(\mu_{k+1})_{\mathcal{A}_k}$ from the system (2.8) and therefore solving a system of reduced dimensions with the following coefficient matrix

$$J_{k,red} = \begin{bmatrix} M & 0 & -L^T \\ 0 & \nu M_{\mathcal{A}_k,\mathcal{A}_k} & M_{\mathcal{A}_k,:} \\ -L & M_{:,\mathcal{A}_k} & 0 \end{bmatrix},$$

where $M_{\mathcal{C}_r,\mathcal{C}_c}$ is the submatrix of M obtained by taking the rows whose indices belong to the set $\mathcal{C}_r$ and the columns whose indices belong to the set $\mathcal{C}_c$. Here, ':' denotes the set of all indices $1, \ldots, n_h$. However, the authors of [34] preferred to work with the full 3×3 block system,

$$J_F := \begin{bmatrix} M & 0 & -L^T \\ 0 & \nu M & M \\ -L & M & 0 \end{bmatrix}, \tag{3.3}$$

[2]We thank Roland Herzog for providing us with all Matlab codes used in [14].

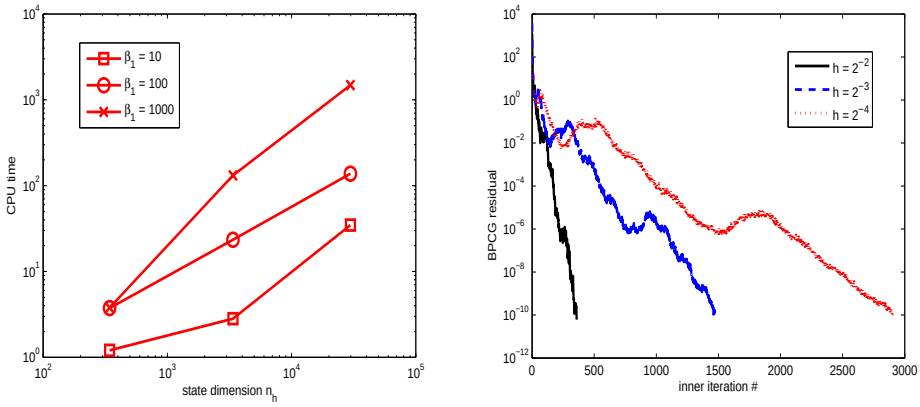

FIG. 3.1. *Unconstrained problem with convection (problem* `CC-pb1` *described in Section 6). Left: CPU time for a single Newton step vs. the discretized state space dimension, for* $\beta = (\beta_1, 0, 0)$ *with* $\beta_1 = 10, 100, 1000$. *Right:* BPCG *residual convergence history for various grid levels* ($\beta_1 = 1000$).

which they considered to be more practical to handle within the semismooth Newton method, than a system whose full dimension depends on the number of indices in the active sets. To solve these complete systems, the following block triangular preconditioner $\mathcal{P}^{BT}$ and inner product matrix $\mathcal{H}$ are introduced in [34]:

$$\mathcal{P}^{BT} = \begin{bmatrix} A_0 & 0 & \cdot \\ 0 & A_1 & 0 \\ -L & M & -S_0 \end{bmatrix}, \qquad \mathcal{H} = \begin{bmatrix} M - A_0 & 0 & 0 \\ 0 & \nu M - A_1 & 0 \\ 0 & 0 & S_0 \end{bmatrix}, \tag{3.4}$$

where A_0 and A_1 are appropriate approximations of M and νM, respectively, so that the matrix $\mathcal{H}$ is positive definite; moreover, $S_0 = LM^{-1}L$ approximates the following true Schur complement of J_F:

$$S_F = LM^{-1}L + \nu^{-1}M. \tag{3.5}$$

Note that the preconditioner $\mathcal{P}^{BT}$ does not depend on the nonlinear iteration k, and therefore on the current active set.

As in the previous approach, the preconditioned system $\left(\mathcal{P}^{BT}\right)^{-1} J_F$ is symmetric and positive definite with respect to the inner product associated with $\mathcal{H}$ and a CG method can be applied. In Section 6 we will report on the performance of the preconditioners $\mathcal{P}^{BT}$, compared with our new preconditioners.

In our analysis, we found the work [24] particularly inspiring, although a simplified setting was considered: a positive definite self-adjoint elliptic operator in the equality constraint, and no bound-constraints. Under these hypotheses, the KKT conditions give a saddle point system with the coefficient matrix J_F in (3.3). In [24] the following factorized approximation to the Schur complement S_F in (3.5) is introduced (the scaling factor $\frac{1}{\nu}$ is omitted):

$$\widehat{S}_F = (\sqrt{\nu}L + M)M^{-1}(\sqrt{\nu}L + M), \tag{3.6}$$

which appears to possess nice independence properties with respect to the problem parameters: the eigenvalues of $\widehat{S}_F^{-1}S_F$ lie in the interval $\left[\frac{1}{2}, 1\right]$ independently of the values of h and ν [24, Theorem 4]. In the following we shall broadly generalize this

idea so as to cover our more complete framework. Optimality results will also be discussed.

The Schur complement approximation (3.6) was also used in [25] in the solution of convection-diffusion (equality constrained) control problems where the authors generalized the above mentioned spectral properties of $\widehat{S}_F^{-1}S_F$ to the case where L is nonsymmetric.

4. A new approximation to the active-set Schur complement. In agreement with other commonly employed preconditioning strategies, the preconditioners we are going to present in Section 5 strongly rely on the quality of the used approximation to the Schur complement of the coefficient matrix J_k. In this section we introduce this approximation and analyze its spectral properties. In the following we shall make great use of the fact that M is a lumped mass matrix, and thus diagonal. This way, M and $\Pi_{\mathcal{A}_k}$ can commute and formulas simplify considerably. To simplify the notation, we shall use the short-hand notation $\Pi_k = \Pi_{\mathcal{A}_k}$.

Using the same partitioning as in (3.1), the *active-set Schur complement* associated with J_k, and its block factorization are given by

$$\begin{aligned} S_k = B_k A^{-1} B_k^T &= \frac{1}{\nu}\begin{bmatrix} \nu L M^{-1} L^T + M & (\alpha_y \nu L M^{-1} - \alpha_u I) P_{\mathcal{A}_k}^T \\ P_{\mathcal{A}_k}(\alpha_y \nu M^{-1} L^T - \alpha_u I) & (\alpha_y^2 \nu + \alpha_u^2) P_{\mathcal{A}_k} M^{-1} P_{\mathcal{A}_k}^T \end{bmatrix} \\ &= \frac{1}{\nu} R_k \begin{bmatrix} \mathbb{S}_k & 0 \\ 0 & (\alpha_y^2 \nu + \alpha_u^2) P_{\mathcal{A}_k} M^{-1} P_{\mathcal{A}_k}^T \end{bmatrix} R_k^T, \end{aligned}$$

with

$$R_k = \begin{bmatrix} I & \frac{1}{\alpha_y^2 \nu + \alpha_u^2}(\alpha_y \nu L M^{-1} - \alpha_u I)\Pi_k M P_{\mathcal{A}_k}^T \\ 0 & I \end{bmatrix}, \tag{4.1}$$

and

$$\mathbb{S}_k = \nu L M^{-1} L^T + M - \frac{1}{\alpha_y^2 \nu + \alpha_u^2}(\alpha_y \nu L M^{-1} - \alpha_u I)\Pi_k M \Pi_k (\alpha_y \nu L M^{-1} - \alpha_u I)^T.$$

We define the following *factorized approximation* of $\mathbb{S}_k$:

$$\widehat{\mathbb{S}}_k := L_1 M^{-1} L_1^T, \qquad \text{with} \quad L_1 = \sqrt{\nu} L \left(I - \gamma_1 \Pi_k\right)^{\frac{1}{2}} + \left(I - \gamma_2 \Pi_k\right)^{\frac{1}{2}} M, \tag{4.2}$$

and

$$\gamma_1 = \frac{\alpha_y^2 \nu}{\alpha_y^2 \nu + \alpha_u^2}, \qquad \gamma_2 = \frac{\alpha_u^2}{\alpha_y^2 \nu + \alpha_u^2}. \tag{4.3}$$

Note that $\gamma_1 + \gamma_2 = 1$, which implies

$$\left(I - \gamma_1 \Pi_k\right)^{\frac{1}{2}} \left(I - \gamma_2 \Pi_k\right)^{\frac{1}{2}} = \sqrt{\gamma_1 \gamma_2}\ \Pi_k + (I - \Pi_k), \tag{4.4}$$

a property that will be used in the sequel. Moreover both (diagonal) matrices under square root have strictly positive diagonal elements for $\gamma_1, \gamma_2 \neq 1$, i.e., for $\alpha_u \neq 0$ and $\alpha_y \neq 0$, respectively. If $\gamma_1 = 1$ (or $\gamma_2 = 1$), then $(I - \gamma_1 \Pi_k)^{\frac{1}{2}}$ (or $(I - \gamma_2 \Pi_k)^{\frac{1}{2}}$) reduces to $(I - \Pi_k)$.

REMARK 4.1. Our approach uses the fact that M is diagonal, both from a computational and a theoretical point of view. If the employed discretization is such

that M is no longer diagonal, then we could define the preconditioner with $\mathrm{diag}(M)$ in place of M. As an alternative, we could keep M in the preconditioner, and solve systems with $P_{\mathcal{A}_k} M^{-1} P_{\mathcal{A}_k}^T$ as discussed in [14, (3.10)], and possibly also approximate the action of M^{-1} by a Chebyshev polynomial [36]. For the sake of simplicity we refrain from further exploring these possibilities.

We proceed with an analysis of the quality of the proposed Schur complement preconditioner.

PROPOSITION 4.2. *Let $\mathbb{S}_k$ and $\widehat{\mathbb{S}}_k$ be as defined above. Then*

$$\widehat{\mathbb{S}}_k = \mathbb{S}_k + \sqrt{\nu}(L(I-\Pi_k) + (I-\Pi_k)L^T).$$

Proof. The result follows from

$$\begin{aligned}\mathbb{S}_k &= \nu L M^{-1} L^T + M - \frac{1}{\alpha_y^2\nu + \alpha_u^2}(\alpha_u^2 \Pi_k M + \alpha_y^2 \nu^2 L \Pi_k M^{-1} L^T - \alpha_y \alpha_u \nu (\Pi_k L^T + L\Pi_k)) \\ &= \nu L(I-\gamma_1\Pi_k)M^{-1}L^T + (I-\gamma_2\Pi_k)M + \sqrt{\nu}(L\sqrt{\gamma_1\gamma_2}\,\Pi_k + \sqrt{\gamma_1\gamma_2}\,\Pi_k L^T),\end{aligned}$$

and

$$\begin{aligned}\widehat{\mathbb{S}}_k &= (\sqrt{\nu}L\,(I-\gamma_1\Pi_k)^{\frac{1}{2}} + (I-\gamma_2\Pi_k)^{\frac{1}{2}}\,M)M^{-1}(\sqrt{\nu}L\,(I-\gamma_1\Pi_k)^{\frac{1}{2}} + (I-\gamma_2\Pi_k)^{\frac{1}{2}}\,M)^T \\ &= \nu L(I-\gamma_1\Pi_k)M^{-1}L^T + (I-\gamma_2\Pi_k)M + \\ &\quad \sqrt{\nu}L\,(I-\gamma_1\Pi_k)^{\frac{1}{2}}\,(I-\gamma_2\Pi_k)^{\frac{1}{2}} + \sqrt{\nu}\,(I-\gamma_1\Pi_k)^{\frac{1}{2}}\,(I-\gamma_2\Pi_k)^{\frac{1}{2}}\,L^T \\ &= \nu L(I-\gamma_1\Pi_k)M^{-1}L^T + (I-\gamma_2\Pi_k)M + \\ &\quad +\sqrt{\nu}L\,(\sqrt{\gamma_1\gamma_2}\,\Pi_k + (I-\Pi_k)) + \sqrt{\nu}\,(\sqrt{\gamma_1\gamma_2}\,\Pi_k + (I-\Pi_k))\,L^T,\end{aligned}$$

where (4.4) was used. ∎

Note that the difference between the true and the approximate Schur complement does not depend on the γ's. The following special case of Proposition 4.2 occurs when all indices are active, so that $\Pi_k = I$.

COROLLARY 4.3. *If $\mathcal{A}_k = \{1, \ldots, n_h\}$, then $\widehat{\mathbb{S}}_k = \mathbb{S}_k$.*

The Schur complement approximation specializes when particular choices of α_u and α_v are made. In the CC case, that is for $(\alpha_u, \alpha_y) = (1, 0)$, we obtain

$$L_1 = \sqrt{\nu}L + (I-\Pi_k)M.$$

In the case of L symmetric and no bound constraints, that is for $\mathcal{A}_k = \emptyset$, we obtain $L_1 = \sqrt{\nu}L + M$, which corresponds to the factor in (3.6), as introduced in [24]. In the Mixed Constraints case, that is for $(\alpha_u, \alpha_y) = (\epsilon, 1)$, we obtain

$$L_1 = \sqrt{\nu}L\left(I - \frac{1}{1+\gamma}\Pi_k\right)^{\frac{1}{2}} + \left(I - \frac{\gamma}{1+\gamma}\Pi_k\right)^{\frac{1}{2}} M,$$

with $\gamma = \epsilon^2/\nu$. Note that both (diagonal) matrices under square root have strictly positive diagonal elements for $\gamma > 0$. Finally, in the pure State Constraints case, i.e. for $(\alpha_u, \alpha_y) = (0, 1)$, we obtain

$$L_1 = \sqrt{\nu}L\,(I-\Pi_k) + M.$$

In the next proposition we derive general estimates for the inclusion interval for the eigenvalues of the pencil $(\mathbb{S}_k, \widehat{\mathbb{S}}_k)$, whose extremes depend on the spectral properties of the nonsymmetric matrix L and on M, for general $\mathcal{A}_k$. Special cases will then be singled out.

PROPOSITION 4.4. *Assume that $\widehat{\mathbb{S}}_k$ is nonsingular. Let*

$$G_k := F(I - \Pi_k) + (I - \Pi_k)F^T, \tag{4.5}$$

where $F = \sqrt{\nu} M^{-\frac{1}{2}} L M^{-\frac{1}{2}}$, with F nonsingular, and

$$H_k := F(I - \gamma_1 \Pi_k)F^T + (I - \gamma_2 \Pi_k) + \sqrt{\gamma_1 \gamma_2}(F\Pi_k + \Pi_k F^T), \tag{4.6}$$

with γ_1, γ_2 as defined in (4.3). Then

$$\alpha_{\min} := \min_{z \neq 0} \frac{z^T G_k z}{z^T H_k z} > -1, \tag{4.7}$$

and the eigenvalues λ of the pencil $(\mathbb{S}_k, \widehat{\mathbb{S}}_k)$ satisfy $\lambda \in \left[\frac{1}{2}, \frac{1}{1+\alpha_{\min}}\right]$.

Proof. For the sake of readability, we omit the subscript k within this proof. The matrix H in (4.6) satisfies $H = M^{-\frac{1}{2}} \mathbb{S} M^{-\frac{1}{2}}$. Let

$$\widehat{H} = M^{-\frac{1}{2}} \widehat{\mathbb{S}} M^{-\frac{1}{2}}. \tag{4.8}$$

Then by Proposition 4.4 we have that G, H in (4.5) and (4.6) satisfy $\widehat{H} = H + G$. Therefore the problem $\mathbb{S}x = \lambda \widehat{\mathbb{S}} x$ can be written as $Hz = \lambda(H + G)z$, with $z = M^{\frac{1}{2}} x$, and for $z \neq 0$ we can write

$$\lambda = \frac{1}{1 + \frac{z^T G z}{z^T H z}}.$$

For $z \neq 0$ we have $\frac{z^T G z}{z^T H z} > -1$ if and only if $z^T(G + H)z > 0$. The latter inequality is satisfied since $G + H = M^{-\frac{1}{2}} \widehat{\mathbb{S}} M^{-\frac{1}{2}}$, and $\widehat{\mathbb{S}}$ is positive definite. This proves the upper bound for λ.

To prove the lower bound, we first consider the case $\gamma_2 \neq 1$. We define $W := (I - \gamma_2 \Pi)^{-\frac{1}{2}} F (I - \gamma_1 \Pi)^{\frac{1}{2}}$ and notice that

$$(I - \gamma_2 \Pi)^{-\frac{1}{2}} \widehat{H} (I - \gamma_2 \Pi)^{-\frac{1}{2}} = (W + I)(W + I)^T,$$

while

$$\begin{aligned}
&(I - \gamma_2 \Pi)^{-\frac{1}{2}} H (I - \gamma_2 \Pi)^{-\frac{1}{2}} \\
&= WW^T + I + \sqrt{\gamma_1 \gamma_2} \left(W\Pi (I - \gamma_1 \Pi)^{-\frac{1}{2}} (I - \gamma_2 \Pi)^{-\frac{1}{2}} + (I - \gamma_2 \Pi)^{-\frac{1}{2}} (I - \gamma_1 \Pi)^{-\frac{1}{2}} \Pi W^T \right) \\
&= WW^T + I + (W\Pi + \Pi W^T),
\end{aligned}$$

where the relation (4.4) was used. For $x \neq 0$ we can thus write

$$\lambda = \frac{x^T \mathbb{S} x}{x^T \widehat{\mathbb{S}} x} = \frac{y^T (WW^T + I + (W\Pi + \Pi W^T))y}{y^T (W + I)(W + I)^T y},$$

where $y = (I - \gamma_2\Pi)^{\frac{1}{2}} M^{\frac{1}{2}} x$. Therefore, $\lambda \geq \frac{1}{2}$ if and only if

$$\frac{y^T(WW^T + I + (W\Pi + \Pi W^T))y}{y^T(W+I)(W+I)^T y} \geq \frac{1}{2}$$

which is equivalent to

$$\frac{1}{2} y^T(WW^T + I + W(2\Pi - I) + (2\Pi - I)W^T)y \geq 0.$$

Noticing that $I = (2\Pi - I)(2\Pi - I)$, it holds

$$WW^T + I + W(2\Pi - I) + (2\Pi - I)W^T = (W + (2\Pi - I))(W + (2\Pi - I))^T \succeq 0;$$

Therefore, the last inequality is always verified, proving the lower bound for λ.

Consider now the case $\gamma_2 = 1$ (which implies $\gamma_1 = 0$). We define $W := F^{-1}(I - \Pi)$. For $x \neq 0$ we can write

$$\lambda = \frac{x^T \mathbb{S} x}{x^T \widehat{\mathbb{S}} x} = \frac{z^T(FF^T + (I-\Pi))z}{z^T(F + (I-\Pi))(F + (I-\Pi))^T z} = \frac{y^T(WW^T + I)y}{y^T(W+I)(W+I)^T y},$$

where $z = M^{\frac{1}{2}} x$ and $y = F^T z$. As above, $\lambda \geq \frac{1}{2}$ if and only if

$$\frac{y^T(WW^T + I)y}{y^T(W+I)(W+I)^T y} \geq \frac{1}{2}$$

which holds since $2(WW^T + I) - (W+I)(W+I)^T = (W-I)(W-I)^T \succeq 0$. □

Proposition 4.4 reformulates the eigenvalue problem with the preconditioned Schur complement in terms of the eigenvalue problem with a different Rayleigh quotient, which seems to be easier to interpret. Numerical experiments confirm the sharpness of the lower extreme (see below); for the upper bound more insightful estimates can be given under additional hypotheses, and these are explored in the following.

COROLLARY 4.5. [25, Theorem 4.1] *Assume $L + L^T \succeq 0$ and let $\mathcal{A}_k = \emptyset$. Then the eigenvalues λ of the pencil $(\mathbb{S}_k, \widehat{\mathbb{S}}_k)$ satisfy $\lambda \in \left[\frac{1}{2}, 1\right]$.*

The result of Corollary 4.5 generalizes the result of [24] to nonsymmetric and positive semidefinite L, showing the optimality and robustness of the approximation with respect to the problem parameters.

To be able to analyze another interesting special case, we first need an auxiliary lemma whose proof is postponed to the appendix.

LEMMA 4.6. *Let $F \in \mathbb{R}^{n\times n}$ be such that $F + F^T \succeq 0$. Then*
i) $\|(F+I)^{-1}(F-I)\| \leq 1$;
ii) $\|(F+I)^{-1}(F+F^T)(F+I)^{-T}\| \leq \frac{1}{2}$.

We can now estimate the eigenvalues of $(\mathbb{S}_k, \widehat{\mathbb{S}}_k)$ for a particular choice of γ_1, γ_2.

PROPOSITION 4.7. *Assume $L + L^T \succeq 0$ and let $\gamma_1 = \gamma_2 = \frac{1}{2}$. Then the eigenvalues λ of the pencil $(\mathbb{S}_k, \widehat{\mathbb{S}}_k)$ satisfy $\lambda \in \left[\frac{1}{2}, 3\right]$.*

Proof. For the sake of readability, we omit the subscript k within this proof. We only have to prove the upper bound. Let $F = \sqrt{\nu} M^{-\frac{1}{2}} L M^{-\frac{1}{2}}$, so that $F + F^T \succeq 0$. Proceeding as in the proof of Proposition 4.4, the eigenproblem $\mathbb{S}x = \lambda \widehat{\mathbb{S}} x$ can be transformed into

$$Hy = \lambda(H + G)y, \tag{4.9}$$

with $y = M^{\frac{1}{2}}x$, where H and G are given in (4.6) and (4.5), respectively. For $\gamma_1 = \gamma_2 = \frac{1}{2}$, we have $H + G = (F + I)\left(I - \frac{1}{2}\Pi\right)(F + I)^T$, while $H = (F - I)\left(I - \frac{1}{2}\Pi\right)(F - I)^T + F + F^T$, which can be readily verified. Therefore, problem (4.9) can be written as

$$\left((F - I)\left(I - \frac{1}{2}\Pi\right)(F - I)^T + F + F^T\right) y = \lambda(F + I)\left(I - \frac{1}{2}\Pi\right)(F + I)^T y,$$

or equivalently, with $u = (F + I)^T y$, as

$$(F + I)^{-1}\left((F - I)\left(I - \frac{1}{2}\Pi\right)(F - I)^T + F + F^T\right)(F + I)^{-T}u = \lambda(I - \frac{1}{2}\Pi)u. \quad (4.10)$$

We then multiply (4.10) from the left by $u^T \neq 0$,

$$u^T(F + I)^{-1}\left((F - I)\left(I - \frac{1}{2}\Pi\right)(F - I)^T + F + F^T\right)(F + I)^{-T}u = \lambda u^T(I - \frac{1}{2}\Pi)u, \quad (4.11)$$

and we note that $u^T\left(I - \frac{1}{2}\Pi\right)u \geq \frac{1}{2}\|u\|^2$. Moreover, using Lemma 4.6

$$u^T(F + I)^{-1}(F - I)\ (I - \frac{1}{2}\Pi)(F - I)^T(F + I)^{-T}u \leq \|\left(I - \frac{1}{2}\Pi\right)\|\|(F - I)^T(F + I)^{-T}\|^2\|u\|^2 \leq \|u\|^2,$$

and $u^T(F + I)^{-1}(F + F^T)(F + I)^{-T}u \leq \frac{1}{2}\|u\|^2$. Therefore, using these last bounds in (4.11) we obtain $\|u\|^2 + \frac{1}{2}\|u\|^2 \geq \lambda\frac{1}{2}\|u\|^2$, with $\|u\| \neq 0$, from which the upper estimate follows. □

In the notation of Proposition 4.4, for $\gamma_1 = \gamma_2$ we bounded $\alpha_{\min}$ by $-\frac{2}{3}$.

REMARK 4.8. The case $\gamma_1 = \gamma_2$ comprises MC problems where $\alpha_u = \epsilon$ and $\alpha_y = 1$, so that the equality $\nu = \epsilon^2$ holds. Therefore, for $\nu = \epsilon^2$ Proposition 4.7 ensures a clustered spectrum of the preconditioned Schur complement, and this also strongly influences the spectrum of the overall preconditioned matrix - see Section 5 - predicting fast convergence of the iterative methods. From an application perspective, these experiments show that if $\nu \approx \epsilon^2$ in the given model, then a good performance of the solver is expected.

The good behavior for $\nu = \epsilon^2$ discussed in the remark above is confirmed by our numerical experiments (see Example 6.4), where problems with MC constraints (1.3) are tested for all combinations of values of ν and ϵ: the best performance is indeed obtained for $\nu = \epsilon^2$. It is also interesting to observe that our findings are in agreement with similar experimental observations reported in [2], where the case $\nu \approx \epsilon^2$ ensured the best performance of a multigrid solver for the MC problem.

Tables 4.1-4.3 display the spectral intervals for $\widehat{\mathbb{S}}_k^{-1}\mathbb{S}_k$ for the three considered model problems (see Table 6.1). In all tables, the minimum and maximum eigenvalues are reported for the kth iteration for which $\lambda_{\max}(\widehat{\mathbb{S}}_k^{-1}\mathbb{S}_k)$ is maximum. The CC case shows the largest, though still extremely modest, dependence of $\lambda_{\max}$ on the problem

parameters, and this dependence quickly fades as β_1 increases. On the other hand, $\lambda_{\min}$ remains largely insensitive to parameter variations, with a small benign increase from the bound $\frac{1}{2}$ for $\nu = 10^{-2}$ as β_1 grows. In the mixed case and $\nu = \epsilon^2$, $\lambda_{\max}$ remains well below the upper estimate 3, for a variety of mesh parameter values.

		$\nu = 10^{-2}$				$\nu = 10^{-6}$			
β_1	h	k	$\lvert\mathcal{I}^k\rvert$	$\lambda_{\min}$	$\lambda_{\max}$	k	$\lvert\mathcal{I}^k\rvert$	$\lambda_{\min}$	$\lambda_{\max}$
0	2^{-2}	1	98	0.51	1.24	3	25	0.55	4.7
	2^{-3}	3	895	0.51	1.27	17	24	0.5	13.14
10	2^{-2}	1	73	0.64	1.18	5	57	0.54	5.32
	2^{-3}	1	891	0.61	1.24	6	44	0.50	10.72
100	2^{-2}	1*	0	1	1	4	49	0.51	4.82
	2^{-3}	1	120	0.95	1.01	6	201	0.5	6.64
1000	2^{-2}	1*	0	1	1	2	49	0.6	1.39
	2^{-3}	1*	0	1	1	2	675	0.58	1.63

* Newton terminates in 2 steps.

TABLE 4.1

Control-Constraints: Extreme eigenvalues of $\widehat{\mathbb{S}}_k^{-1}\mathbb{S}_k$, Newton iteration k, and dimension of the Inactive set, $|\mathcal{I}^k|$, as the mesh size h, the regularization parameter ν and the convection parameter $\beta = (\beta_1, 0, 0)$ vary.

		$\nu = 10^{-2}$					$\nu = 10^{-6}$				
β_1	h	ϵ	k	$\lvert\mathcal{I}^k\rvert$	$\lambda_{\min}$	$\lambda_{\max}$	ϵ	k	$\lvert\mathcal{I}^k\rvert$	$\lambda_{\min}$	$\lambda_{\max}$
0	2^{-2}	10^{-1}	1	196	0.53	1.10	10^{-1}	2	165	0.64	1.97
		10^{-2}	1	294	0.51	1.51	10^{-2}	1	196	0.75	1.10
		10^{-3}	2	303	0.50	1.93	10^{-3}	1	196	0.75	1.01
	2^{-3}	10^{-1}	2	2242	0.52	1.16	10^{-1}	3	1212	0.51	2.63
		10^{-2}	3	2782	0.51	1.97	10^{-2}	1	1800	0.51	1.29
		10^{-3}	3	3030	0.51	3.37	10^{-3}	1	1800	0.51	1.03
10	2^{-2}	10^{-1}	1	315	0.53	1.05	10^{-1}	2	147	0.57	3.28
		10^{-2}	0*	343	0.53	0.93	10^{-2}	1	196	0.69	1.37
		10^{-3}	0*	343	0.53	0.93	10^{-3}	1	196	0.69	1.03
	2^{-3}	10^{-1}	1	2549	0.56	1.18	10^{-1}	3	1406	0.50	5.20
		10^{-2}	1	3135	0.53	1.55	10^{-2}	2	1631	0.50	1.71
		10^{-3}	1	3303	0.53	2.45	10^{-3}	1	1800	0.50	1.08
100	2^{-2}	10^{-1}	0*	343	0.84	0.98	10^{-1}	2	196	0.51	4.40
		10^{-2}	0*	343	0.84	0.98	10^{-2}	2	196	0.51	2.49
		10^{-3}	0*	343	0.84	0.98	10^{-3}	1	147	0.51	1.24
	2^{-3}	10^{-1}	1	3299	0.84	1.01	10^{-1}	2	1575	0.50	5.9
		10^{-2}	1	3367	0.84	1.12	10^{-2}	2	1519	0.50	3.25
		10^{-3}	0*	3375	0.84	0.99	10^{-3}	2	1800	0.50	1.42
1000	2^{-2}	10^{-1}	0*	343	0.98	0.99	10^{-1}	1	294	0.51	1.22
		10^{-2}	0*	343	0.98	0.99	10^{-2}	1	294	0.51	1.22
		10^{-3}	0*	343	0.98	0.99	10^{-3}	1	294	0.52	1.24
	2^{-3}	10^{-1}	0*	3375	0.98	0.99	10^{-1}	2	2475	0.52	1.40
		10^{-2}	0*	3375	0.98	0.99	10^{-2}	2	2644	0.52	1.34
		10^{-3}	0*	3375	0.98	0.99	10^{-3}	2	2925	0.51	1.31

* Newton terminates in 1 step.

TABLE 4.2

Mixed-Constraints: Extreme eigenvalues of $\widehat{\mathbb{S}}_k^{-1}\mathbb{S}_k$, Newton iteration k, and dimension of the Inactive set, $|\mathcal{I}^k|$, as the mesh size h, the regularization parameters ν, ϵ and the convection parameter $\beta = (\beta_1, 0, 0)$ vary.

The dependence of $\lambda_{\max}$ on the parameters in the CC and SC cases can be analyzed by using the following result, whose proof is postponed to the appendix.

PROPOSITION 4.9. *Let λ be an eigenvalue of $\widehat{\mathbb{S}}_k^{-1}\mathbb{S}_k$. Then in the CC and SC*

		$\nu = 10^{-2}$				$\nu = 10^{-6}$			
β_1	h	k	$\lvert\mathcal{I}^k\rvert$	$\lambda_{\min}$	$\lambda_{\max}$	k	$\lvert\mathcal{I}^k\rvert$	$\lambda_{\min}$	$\lambda_{\max}$
0	2^{-2}	2	303	0.50	2.01	1	196	0.75	1.00
	2^{-3}	3	3030	0.51	3.65	1	1800	0.51	1.02
10	2^{-2}	0*	343	0.53	0.93	1	196	0.69	1.02
	2^{-3}	1	3319	0.52	2.94	1	1800	0.50	1.06
100	2^{-2}	0*	343	0.84	0.98	1	196	0.50	1.23
	2^{-3}	0*	3375	0.84	0.99	2	2250	0.50	1.56
1000	2^{-2}	0*	343	0.98	0.99	0*	343	0.51	0.84
	2^{-3}	0*	3375	0.98	0.99	0*	3375	0.51	0.91

* Newton terminates in 1 step.

TABLE 4.3

State-Constraints: Extreme eigenvalues of $\widehat{\mathbb{S}}_k^{-1}\mathbb{S}_k$, Newton iteration k, and dimension of the Inactive set, $|\mathcal{I}^k|$, as the mesh size h, the regularization parameter ν and the convection parameter $\beta = (\beta_1, 0, 0)$ vary.

case it holds

$$\lambda \leq \zeta^2 + (1+\zeta)^2,$$

with
i) If $(\alpha_u, \alpha_y) = (1, 0)$ (CC case), then $\zeta = \|M^{\frac{1}{2}} \left(\sqrt{\nu}L + M(I-\Pi)\right)^{-1} \sqrt{\nu}LM^{-\frac{1}{2}}\|$; Moreover, if $L + L^T \succ 0$, then for $\nu \to 0$, ζ is bounded by a constant independent of ν;
ii) If $(\alpha_u, \alpha_y) = (0, 1)$ (SC case), then $\zeta = \|(I + \sqrt{\nu}M^{-\frac{1}{2}}LM^{-\frac{1}{2}}(I-\Pi_k))^{-1}\|$; Moreover, $\zeta \to 1$ for $\nu \to 0$.

The boundedness of ζ as $\nu \to 0$ in both the CC and SC cases justifies the good behavior of the eigenvalues shown in Tables 4.1 and 4.3.

5. New preconditioners for the active-set Newton method. In this section we propose two classes of preconditioners, which can be used throughout the nonlinear iterations, and automatically modified as the system dimensions dynamically change due to the different number of active indices. More precisely, for the problem partitioned as in (3.1) we consider the following block diagonal preconditioner $\mathcal{P}_k^{BDF}$, and indefinite preconditioner $\mathcal{P}_k^{IPF}$:

$$\mathcal{P}_k^{BDF} = \begin{bmatrix} A & 0 \\ 0 & \widehat{S}_k \end{bmatrix}, \tag{5.1}$$

and

$$\mathcal{P}_k^{IPF} = \begin{bmatrix} I & 0 \\ B_k A^{-1} & I \end{bmatrix} \begin{bmatrix} A & 0 \\ 0 & -\widehat{S}_k \end{bmatrix} \begin{bmatrix} I & A^{-1}B_k^T \\ 0 & I \end{bmatrix}, \tag{5.2}$$

where in both cases, the matrix $\widehat{S}_k$ is factorized as

$$\widehat{S}_k = \frac{1}{\nu} R_k \begin{bmatrix} \widehat{\mathbb{S}}_k & 0 \\ 0 & (\alpha_y^2\nu + \alpha_u^2) P_{\mathcal{A}_k} M^{-1} P_{\mathcal{A}_k}^T \end{bmatrix} R_k^T,$$

with $\widehat{\mathbb{S}}_k = L_1 M^{-1} L_1^T$, and R_k and L_1 given in (4.1) and (4.2), respectively. The following result can be readily proved from Proposition 4.4.

PROPOSITION 5.1. *Assume that $\widehat{\mathbb{S}}_k$ is nonsingular and let $\alpha_{\min}$ be as defined in (4.7). Then the eigenvalues λ of the pencil $(J_k, \mathcal{P}_k^{BDF})$ satisfy*

$$\lambda\left(J_k,\ \mathcal{P}_k^{BDF}\right) \in \left\{1,\ \frac{1 \pm \sqrt{5}}{2}\right\} \cup I^- \cup I^+,$$

where

$$I^- = \left[\frac{1}{2}\left(1 - \sqrt{1 + \frac{4}{(1+\alpha_{\min})^2}}\right),\ \frac{1-\sqrt{2}}{2}\right],\ I^+ = \left[\frac{1+\sqrt{2}}{2},\ \frac{1}{2}\left(1 + \sqrt{1 + \frac{4}{(1+\alpha_{\min})^2}}\right)\right].$$

The eigenvalues λ of the pencil $(J_k, \mathcal{P}_k^{IPF})$ satisfy

$$\lambda(J_k, \mathcal{P}_k^{IPF}) \in \{1\} \cup \left[\frac{1}{2}, \frac{1}{1+\alpha_{\min}}\right].$$

Proof. We observe that the pencil $\left(J_k,\ \mathcal{P}_k^{BDF}\right)$ has the same eigenvalues as:

$$\left(\mathcal{P}_k^{BDF}\right)^{-1/2} J_k \left(\mathcal{P}_k^{BDF}\right)^{-1/2} = \begin{bmatrix} I & A^{-1/2} B_k^T \widehat{S}_k^{-1/2} \\ \widehat{S}_k^{-1/2} B_k A^{-1/2} & 0 \end{bmatrix}.$$

Using [12, Lemma 2.1], the eigenvalues of the pencil $(J_k,\ \mathcal{P}_k^{BDF})$ are either 1 or have the form $\frac{1}{2}\left(1 \pm \sqrt{1+4\sigma^2}\right)$, where σ is a singular value of $\widehat{S}_k^{-1/2} B_k A^{-1/2}$, that is, σ^2 is an eigenvalue of $\widehat{S}_k^{-1} S_k$. Considering that $\operatorname{spec}\left(\widehat{S}_k^{-1} S_k\right) = \{1\} \cup \operatorname{spec}\left(\widehat{\mathbb{S}}_k^{-1} \mathbb{S}_k\right)$, we have

$$\lambda\left(J_k,\ \mathcal{P}_k^{BDF}\right) \in \left\{1, \frac{1 \pm \sqrt{5}}{2}\right\} \cup \left\{\frac{1}{2}\left(1 \pm \sqrt{1+4\sigma^2}\right) \mid \sigma^2 \in \operatorname{spec}\left(\widehat{\mathbb{S}}_k^{-1} \mathbb{S}_k\right)\right\}.$$

The claim thus follows from Proposition 4.3.

As for the pencil $\left(J_k,\ \mathcal{P}_k^{IPF}\right)$, we have the factorization

$$\left(\mathcal{P}_k^{IPF}\right)^{-1} J_k = \begin{bmatrix} I & -A^{-1}B_k \\ 0 & I \end{bmatrix} \begin{bmatrix} I & 0 \\ 0 & \widehat{S}_k^{-1} S_k \end{bmatrix} \begin{bmatrix} I & A^{-1}B_k \\ 0 & I \end{bmatrix}. \tag{5.3}$$

Again, the result follows from Proposition 4.4. ∎

Under the stated hypotheses, refined bounds for the eigenvalues of the indefinitely preconditioned problem can be derived using the bounds for the eigenvalues of $\widehat{\mathbb{S}}_k^{-1} \mathbb{S}_k$ obtained in Corollary 4.5, Proposition 4.7 and Proposition 4.9.

In the case of indefinite preconditioning, the preconditioned matrix $\left(\mathcal{P}_k^{IPF}\right)^{-1} J_k$ has real spectrum, however it is no longer symmetric so that in general, a nonsymmetric solver needs to be applied. In our numerical experiments we used GMRES [29], for which it is known that the eigenvalues alone may not be sufficient to predict convergence, but that also eigenvectors play a role. In addition, indefinite preconditioners are often plagued by the presence of Jordan blocks, whose sensitivity may influence the use of inexact strategies; see, e.g., [31] for a detailed discussion. Fortunately, since the (1,1) block of J_k is reproduced exactly in the preconditioner, in our setting the

spectral structure is considerably simplified, and in particular, Jordan blocks do not occur. The following proposition determines the complete eigenvector decomposition of the preconditioned matrix.

PROPOSITION 5.2. *Let* $\widehat{S}_k^{-1} S_k X = X\Lambda$ *be the eigendecomposition of* $\widehat{S}_k^{-1} S_k$, *with* $X = [X_1, X_2]$ *and* $\Lambda = \mathrm{blkdiag}(I, \Lambda_2)$ *partitioned so that* X_1 *contains the eigenvectors corresponding to the unit eigenvalue. Then the preconditioned matrix* $\left(\mathcal{P}_k^{IPF}\right)^{-1} J_k$ *admits the following eigenvalue decomposition*

$$\left(\mathcal{P}_k^{IPF}\right)^{-1} J_k = Q \begin{bmatrix} I & & \\ & I & \\ & & \Lambda_2 \end{bmatrix} Q^{-1},$$

with

$$Q = \left[\begin{array}{c|c|c} I & 0 & -A^{-1}B_k X_2 \\ 0 & X_1 & X_2 \end{array}\right], \qquad Q^{-1} = \left[\begin{array}{c|c} I & A^{-1}B_k X_2 X_2^T \widehat{S}_k \\ 0 & X_1^T \widehat{S}_k \\ 0 & X_2^T \widehat{S}_k \end{array}\right].$$

Proof. Writing

$$\left(\mathcal{P}_k^{IPF}\right)^{-1} J_k = \begin{bmatrix} I & A^{-1}B_k(I - \widehat{S}_k^{-1} S_k) \\ 0 & \widehat{S}_k^{-1} S_k \end{bmatrix},$$

the decomposition can be explicitly verified upon substitution. The nonsingularity of Q follows from that of $X = [X_1, X_2]$. The inverse of Q can be derived by observing that X can be chosen so that $X^T \widehat{S}_k X = I$. □

The explicit form of Proposition 5.2 allows one to use standard results to bound the GMRES residual norm, by providing bounds for the norm of Q and its inverse Q^{-1}, and exploiting the fact that the spectrum of the preconditioned matrix is real (see, e.g., [28, Prop. 6.32]).

6. Numerical experiments. In this section we provide a detailed performance analysis of the proposed preconditioners $\mathcal{P}_k^{IPF}$ in (5.2) and $\mathcal{P}_k^{BDF}$ in (5.1) for the active-set Newton method and use problems with constraints in (1.2)-(1.4) as prototypical problems. In particular, the analysis of the pure State Constraints case (1.4) will be analyzed as the limit case of the MC constraints (1.3) for $\epsilon \to 0$.

label	Ω	a	b	y_d
`CC-Pb1`	$(-1,1)^3$	0	2.5	1 for $\lvert x_1\rvert \le \frac{1}{2}$, -2 otherwise
`CC-Pb2`	$(0,1)^3$	$\frac{1}{10}\exp(-\lVert x\rVert^2)$	$\frac{1}{2}$	$\exp(-64\lVert x - \frac{1}{2}\rVert^2)$
`MC-Pb1`	$(-1,1)^3$	$-\infty$	0	1 for $\lvert x_1\rvert \le \frac{1}{2}$, -2 otherwise

TABLE 6.1
Problem data for the numerical experiments. Here $x = (x_1, x_2, x_3) \in \Omega$.

In all our examples, we use the three-dimensional data for the discretized problem generated by the codes in [14]. The matrices stem from the discretization by upwind finite differences on a uniform three-dimensional grid (so that $L + L^T \succ 0$). Zero Dirichlet boundary conditions, that is $\bar{y} = 0$ in (1.1), were used throughout. We stress that for large convection and in the presence of boundary layers, other discretizations may be more suitable; we refer to the recent nice essay by Stynes on the pros and cons

of different approaches [35]. We also notice that different discretization techniques will lead to coefficient matrices L with possibly quite different spectral properties.

In Table 6.1 information on the data used in our numerical experiments can be found, for two test cases with control constraints, and one test case for mixed and state constraints; here $x = (x_1, x_2, x_3)$ is an element of Ω. The mesh parameter in each direction was taken as $h \in \{2^{-2}, 2^{-3}, 2^{-4}, 2^{-5}\}$ which corresponds to a dimension for the state or control vectors $n_h \in \{343, 3375, 29791, 250047\}$. The total linear system dimension is thus between $3n_h$ and $4n_h$, depending on the number of indices in the active set at each Newton iteration.

6.1. Algorithmic considerations. Throughout this section we consider the implementation of the active-set Newton method with the following solvers and preconditioning strategies:

AS-GMRES-IPF	Active-set Newton method with linear solver GMRES preconditioned with $\mathcal{P}_k^{IPF}$;
AS-MINRES-BDF	Active-set Newton method with linear solver MINRES preconditioned with $\mathcal{P}_k^{BDF}$;
AS-BPCG-BT	Variant of active-set Newton method as proposed in [34], with BPCG preconditioned with $\mathcal{P}^{BT}$ defined in (3.4).

The application of the Schur complement approximation $\widehat{\mathbb{S}}_k$ requires solving with L_1 and its transpose in (4.2). These solves were replaced by the use of an algebraic multigrid operator (HSL-MI20, [3]), which needs to be recomputed at each Newton iteration. HSL-MI20 is used with all default parameters except for the value `control.st_parameter`=10^{-4}. Moreover, we set the number of pre/post smoothing steps equal to 5 for all the experiments with the MC problems, while with CC problems only for the finest mesh $h = 2^{-5}$. Although in most cases satisfactory results were obtained with this software, we did experience some anomalous behavior when strong convection was used. In these cases, ad-hoc algebraic multigrid strategies should be adopted. We also recall that both Π_k and M are diagonal, therefore L_1 is obtained from the convection-diffusion matrix by scaling, and then modifying its diagonal.

According to [36], we used $A_0 = 0.9M$ and $A_1 = 0.9(\nu\, M)$ for the parameterized preconditioners in (3.4) within the BPCG iteration. Systems with L to apply S_0 in (3.4) are approximately solved with the aforementioned HSL-MI20 code.

We set a limit of 80 GMRES iterations and 1000 MINRES and BPCG iterations. If a solver reaches the maximum number of iterations, the last computed iterate is used as the next Newton iterate.

As for the nonlinear iteration, in all tests we set the parameter c in the definition of the active-set strategy (2.7) equal to one, and we use a null starting guess x_0 in the Newton iteration, which by (2.7) implies that $\mathcal{A}_0 = \emptyset$ in all settings. As already mentioned, we used the stopping criterion (2.10) with $\eta_k = \eta_k^E$ in (2.11) where we further included the safeguard $\tau_s = 10^{-10}$ as follows

$$\|J_k x_{k+1}^{j_*} - f_k\| = \max\{\tau_s, \eta_k^E \|J_k x_{k+1}^0 - f_k\|\}, \tag{6.1}$$

$k \geq 1$, with the tight tolerance $\tau_1 = 10^{-10}$ in (2.11) [9]. While the residual 2-norm in (6.1) can be cheaply evaluated for GMRES when using right preconditioning, in the case of MINRES we explicitly computed the (unpreconditioned) residual vector at each iteration, and then computed its norm; for MINRES we thus slightly modified the code available in [10].

In the numerical tests in Section 6.2.3 we also experimented with the adaptive choice $\eta_k = \eta_k^I$ in (2.12), with $\tau_2 = 10^{-4}, \tau_3 = 10^{-2}$, together with the above safeguard threshold τ_s. We experimentally verified that this choice of tolerances preserved the global convergence of the active set Newton procedure.

Concerning the outer iteration, we followed [14] and we declare convergence when the nonlinear residual is sufficiently small, i.e.

$$\|F(u_k, y_k, p_k, \mu_k)\| \leq \tau_f, \qquad \text{with} \quad \tau_f = 10^{-8}.$$

We verified that this criterion was equivalent to terminating the iteration as soon as the active sets stay unchanged in two consecutive steps as proved in [1, 20]. On the contrary, any run performing more than 200 nonlinear iterations is considered a failure and will be denoted with the symbol '-' in the forthcoming tables.

All numerical experiments were performed on a 4xAMD Opteron 850, 2.4GHz, 16GB of RAM using Matlab R2012a [19].

6.2. Numerical results. The presentation of the numerical results is organized as follows. Section 6.2.1 is devoted to the comparison of AS-GMRES-IPF and AS-MINRES-BDF with AS-BPCG-BT (see Section 3 and (3.4)) on symmetric CC problems. Section 6.2.2 collects the numerical results of the new proposals AS-GMRES-IPF and AS-MINRES-BDF on symmetric and nonsymmetric problems for a variety of problem parameters. Finally, in Section 6.2.3 an *inexact* active set approach is considered in the solution of nonsymmetric CC problems.

In some cases, a comparative computational analysis is carried out by using performance profiles for a given set of test problems and a given selection of algorithms [8]. For a problem P in our testing set and an algorithm A, we let $\texttt{ti}_{P,A}$ denote the total CPU time employed to solve problem P using algorithm A and $\texttt{ti}_P$ be the total CPU time employed by the *fastest* algorithm to solve problem P. As stated in [8], the CPU time performance profile is defined for algorithm A as

$$\pi_A(\tau) = \frac{\text{number of problems s.t. } \texttt{ti}_{P,A} \leq \tau\, \texttt{ti}_P}{\text{number of problems}}, \quad \tau \geq 1,$$

that is the probability[3] for solver A that a performance ratio $\texttt{ti}_{P,A}/\texttt{ti}_P$ is within a factor τ of the best possible ratio. The function $\pi_A(\tau)$ is the (cumulative) distribution function for the performance ratio.

In the upcoming tables of results the following data will be reported: the average number of linear inner iterations (LI), the number of nonlinear outer iterations (NLI in brackets), the average elapsed CPU time of the inner solver (CPU), and the total elapsed CPU time (TCPU).

Finally, to be able to evaluate the effectiveness of the preconditioned linear solvers, we take as reference the computational cost of solving the whole system with a sparse direct solver ("backslash" in Matlab). For the finest mesh, corresponding to $h = 2^{-5}$, the *compiled* direct solver takes 611 seconds to solve a single linear system with $\mathcal{A}_k = \emptyset$ for some k ($\nu = 10^{-2}, \beta = 0$). We note that this corresponds to the cost of the first iteration when the active set Newton algorithm is applied to every problem of the family (1.1). For comparison purposes, multiplying by the number of nonlinear iterations, the total cost of the process when the inner system is solved with a sparse direct method can be derived.

[3] Or, more precisely, the frequency.

		AS-GMRES-IPF			AS-MINRES-BDF			AS-BPCG-BT		
ν	p	LI (NLI)	CPU	TCPU	LI (NLI)	CPU	TCPU	LI (NLI)	CPU	TCPU
10^{-2}	2	9.6(3)	0.1	0.2	20(3)	0.1	0.2	11.3(3)	0.1	0.2
	3	9.5(4)	0.8	3.2	19.5(4)	1.1	4.2	10.7(4)	0.7	2.7
	4	8.5(4)	1.5	8.5	18.7(4)	2.5	9.9	10.0(4)	6.7	26.8
	5	8.0(4)	12.1	48.2	19.2(4)	36.1	144.4	9.5(4)	17.5	69.9
10^{-4}	2	6.5(7)	0.1	0.11	13.8(7)	0.1	0.2	17.5(7)	0.2	1.3
	3	11.2(11)	0.7	8.1	23.8(11)	1.3	14.4	21.1(11)	1.3	14.7
	4	10.7(17)	1.8	30.1	23.5(17)	3.1	51.6	18.0(17)	4.7	80.1
	5	10.3(15)	16.1	241.4	24.3(15)	31.6	474.3	18.2(15)	30.9	463.3
10^{-6}	2	10.3(9)	0.1	0.2	22.7(9)	0.1	0.35	41.1(9)	0.1	0.7
	3	16.0(19)	1.1	21.5	34.6(19)	1.9	35.8	99.0(19)	6.1	115.6
	4	17.6(54)	2.9	160.7	44.9(54)	5.7	289.8	93.5(54)	13.6	735.6
	5	22.0(68)	38.4	2608.4	56.3(89)	63.2	5627.2	102.1(68)	136.7	9293.6
10^{-8}	2	11.1(9)	0.1	0.2	25.4(9)	0.1	0.4	58.6(9)	0.1	1.0
	3	18.3(27)	0.7	20.2	40.1(27)	2.1	57.6	133.2(27)	8.3	224.1
	4	30.3(74)	7.3	540.5	72.1(66)	9.2	513.4	385.0(66)	60.1	3962.8
	5	-	-	-	-	-	-	-	-	-

TABLE 6.2

Comparison among AS-GMRES-IPF, AS-MINRES-BDF *and* AS-BPCG-BT. *Test problem* `CC-Pb1` *for a variety of* $h = 2^{-p}$ *and* ν *(L symmetric, i.e.,* $\beta = 0$*).*

		AS-GMRES-IPF			AS-MINRES-BDF			AS-BPCG-BT		
ν	p	LI (NLI)	CPU	TCPU	LI (NLI)	CPU	TCPU	LI (NLI)	CPU	TCPU
10^{-2}	2	8.75(4)	0.1	0.2	18(4)	0.1	0.2	10.0(4)	0.03	0.10
	3	8.0(5)	0.2	0.8	16.8(5)	0.9	4.7	9.0(5)	0.2	0.99
	4	7.4(5)	1.3	6.5	16.2(5)	2.2	11.1	9.2(5)	1.8	8.77
	5	7.4(5)	11.3	56.4	16.6(5)	19.4	96.7	8.4(5)	15.2	76.1
10^{-4}	2	11.1(9)	0.1	0.2	23.2(9)	0.1	0.4	28.4(7)	0.1	0.6
	3	12.9(13)	0.3	3.8	27.7(13)	1.5	19.8	24.4(13)	0.5	6.4
	4	13.0(14)	2.1	29.5	28.7(14)	3.7	52.1	20.0(14)	3.6	50.1
	5	11.7(13)	18.5	240.8	27.5(13)	32.0	416.1	20.5(13)	28.2	367.5
10^{-6}	2	12.2(12)	0.1	0.3	26.6(12)	0.1	0.5	52.2(12)	0.1	1.3
	3	16.8(22)	0.4	8.8	36.8(22)	2.0	44.6	115.5(22)	2.1	46.7
	4	18.2(35)	3.1	106.9	43.5(36)	5.7	204.8	118.5(35)	19.3	675.2
	5	20.0(41)	34.6	1416.9	52.5(53)	59.5	3151.9	84.3(40)	109.2	4367.1
10^{-8}	2	10.4(11)	0.1	0.2	23.2(11)	0.1	0.4	64.3(11)	0.1	1.6
	3	15.7(19)	0.4	8.2	35.5(19)	1.9	37.1	195.1(19)	3.8	71.2
	4	27.6(55)	5.3	289.1	69.0(63)	9.1	572.0	360.5(54)	55.9	3021.7
	5	41(156)	90.7	14156.0	-	-	-	343.3(131)	438.2	57406.9

TABLE 6.3

Comparison among AS-GMRES-IPF, AS-MINRES-BDF *and* AS-BPCG-BT. *Test with* `CC-Pb2` *for a variety of* $h = 2^{-p}$ *and* ν *(L symmetric, i.e.,* $\beta = 0$*).*

6.2.1. Comparison with the BPCG approach. In order to make comparisons with AS-BPCG-BT in the setting used in [34], we restrict our testing set to symmetric CC problems `CC-Pb1` and `CC-Pb2` with $\beta = 0$. Numerical results are reported in Tables 6.2 and 6.3. The number of nonlinear iterations remains quite low for most choices of the parameters, except for the finest grid and the limit case $\nu = 10^{-8}$. All methods seem to show some ν-dependence both in the (inner) linear solver, and in the (outer) nonlinear iteration; however, while in both problems for AS-GMRES-IPF and AS-MINRES-BDF such dependence is rather mild, this is significantly more evident for AS-BPCG-BT. Large values of LI for AS-BPCG-BT in the tables correspond to runs where the maximum number of inner iterations is reached. This shortcoming makes AS-BPCG-BT not competitive in almost all parameter combinations, with timings that differ significantly from the other methods, up to at most one order of magnitude. Finally, we recall that at each iteration AS-GMRES-IPF and AS-MINRES-BDF solve linear systems of dimension $3n_h + n_{\mathcal{A}_k}$, whereas AS-BPCG-BT solves systems of fixed dimension $3n_h$. The numbers in Tables 6.2 and 6.3 show that an appropriate explicit treatment of the active-set information within the preconditioner is capable of making

up for the larger problem size, yielding an overall significant gain in CPU time.

REMARK 6.1. For the sake of completeness, we also solved the problem with the block triangular preconditioner suggested in [34], with GMRES as a solver instead of BPCG. Results are reported in Table 6.4 for a selection of parameters and for both problems. The results do not differ from those showed in the previous tables, indicating that the chosen linear solver is not responsible for the unsatisfactory performance of the preconditioned iteration. Because of the use of GMRES, memory requirements are clearly superior to those for BPCG.

		AS-GMRES-BT					
		CC-Pb1			CC-Pb2		
ν	p	LI (NLI)	CPU	TCPU	LI (NLI)	CPU	TCPU
10^{-2}	2	10.7(4)	0.1	0.4	9.25(4)	0.06	0.3
	3	9.8(4)	1.3	5.1	7.8(5)	0.3	1.6
	4	8.5(4)	7.9	31.9	7.6(5)	2.4	12.2
	5	8.5(4)	19.5	77.9	7.2(5)	17.5	87.7
10^{-4}	2	14.1(7)	0.3	2.2	22.0(9)	0.1	0.8
	3	16.5(11)	1.8	20.2	19.9(13)	0.7	8.8
	4	14.2(17)	4.2	71.5	16.5(14)	4.2	59.0
	5	13.9(15)	30.2	452.5	15.8(13)	33.4	433.6
10^{-6}	2	25.1(9)	0.1	0.9	31.3(12)	0.1	1.7
	3	50.6(19)	6.6	125.7	55.6(22)	3.5	77.6
	4	46.9(54)	15.0	810.9	55.3(35)	19.8	691.2
	5	49.7(68)	141.5	9621.7	41.1(40)	117.5	4700.1
10^{-8}	2	27.9(9)	0.1	1.1	37.2(11)	0.2	2.1
	3	56.9(27)	8.6	232.0	75.4(19)	7.6	144.7
	4	115.5(74)	56.7	4134.5	164.8(54)	109.9	5932.9
	5	-	-	-	102.1(120)	507.7	60927.8

TABLE 6.4

Performance results for AS-GMRES-BT. *Test with* `CC-Pb1` *and* `CC-Pb2` *for a variety of* $h = 2^{-p}$ *and* ν *(*L *symmetric, i.e.,* $\beta = 0$*).*

6.2.2. Dependence on the problem parameters. We tested the new preconditioners on CC, MC and SC problems by analyzing their dependence on the parameters of the discretized problem, i.e. the regularization parameter ν, the convection coefficient β, the mesh size h and, for the MC case, the regularization parameter ϵ.

EXAMPLE 6.2. For the CC problems, we varied $h \in \{2^{-2}, 2^{-3}, 2^{-4}, 10^{-5}\}$, $\nu \in \{10^{-2}, 10^{-4}, 10^{-6}, 10^{-8}\}$, and we set $\beta = (\beta_1, 0, 0)$ with $\beta_1 \in \{0, 10, 100, 1000\}$. We remark that $\nu = 10^{-8}$ was included for completeness, however it will be considered as a limit case because it is rather small. Analogously, $\beta_1 = 1000$ makes the operator very convection-dominated, providing anomalous behaviors in some exceptional cases; we did not explore whether for this extreme value of β_1 the upwind discretization was sufficient in these cases to damp the well-known numerical instabilities arising in the discretization phase. In fact, the value $\beta_1 = 1000$ was only considered for consistency with respect to the experiments carried out in [14]. In the same lines, we prefer to limit our speculations on the dependence with respect to β to the empirical level, as a deeper analysis would require a thorough discussion of both the discretization strategy and the employed convection; this is clearly beyond the scope of this paper.

We collect the results obtained with AS-GMRES-IPF and AS-MINRES-BDF for the problems `CC-Pb1` and `CC-Pb2` in Tables 6.5-6.6 and the corresponding total CPU time performance profile is displayed in Figure 6.1 (left plot) varying all the parameters for a total of 128 runs. The average number of inner iterations is quite homogeneous with respect to h and slightly dependent on ν and β. A comparison of Tables 6.5 and 6.6

		$\nu = 10^{-2}$		$\nu = 10^{-4}$		$\nu = 10^{-6}$		$\nu = 10^{-8}$	
β_1	p	LI(NLI)	TCPU	LI(NLI)	TCPU	LI(NLI)	TCPU	LI(NLI)	TCPU
0	2	9.6(3)	0.2	6.5(7)	0.1	10.3(9)	0.2	11.1(9)	0.2
	3	9.5(4)	3.2	11.2(11)	8.0	16.0(19)	21.5	18.3(27)	20.2
	4	8.5(4)	8.5	10.7(17)	30.1	17.6(54)	160.7	30.3(74)	540.5
	5	8.0(4)	48.2	10.3(15)	241.4	22.0(68)	2608.4	-	-
10	2	9.0(3)	0.1	8.3(10)	0.2	10.4(10)	0.3	11.3(10)	0.3
	3	8.5(4)	0.7	10.5(13)	3.0	15.4(18)	6.8	19.8(19)	10.7
	4	8.5(4)	6.1	10.8(13)	25.3	18.6(41)	135.9	23.8(109)	509.1
	5	8.0(4)	53.6	11.0(15)	277.6	20.9(47)	1810.7*	36.9(164)	13203.7*
10^2	2	5.0(3)	0.1	7.0(4)	0.1	10.0(6)	0.1	13.7(8)	0.3
	3	6.0(3)	0.4	9.6(5)	0.9	12.3(12)	3.5	23.7(19)	12.9
	4	5.3(3)	2.9	8.8(6)	8.9	15.1(14)	41.4	34.3(46)	337.9
	5	7.3(3)	40.3	10.0(6)	108.2	14.4(19)	690.5*	40.0(81)	8383.7*
10^3	2	3.0(2)	0.1	4.5(2)	0.1	6.0(4)	0.1	8.8(6)	0.2
	3	4.0(2)	0.2	5.0(2)	0.2	5.8(6)	0.8	16.3(18)	7.6
	4	4.5(2)	1.7	6.5(2)	2.4	8.1(6)	9.1	18.0(14)	53.2
	5	4.5(2)	29.3	5.6(3)	53.5	7.2(7)	156.5	25.0(26)	2517.2*

		$\nu = 10^{-2}$		$\nu = 10^{-4}$		$\nu = 10^{-6}$		$\nu = 10^{-8}$	
β_1	p	LI(NLI)	TCPU	LI(NLI)	TCPU	LI(NLI)	TCPU	LI(NLI)	TCPU
0	2	8.7(4)	0.2	11.1(9)	0.2	12.1(12)	0.4	10.4(11)	0.3
	3	8.0(5)	0.8	12.9(13)	3.8	16.8(22)	8.8	15.7(19)	8.2
	4	7.4(5)	6.5	13.0(14)	29.5	18.2(35)	106.9	27.6(55)	289.1
	5	7.4(5)	56.4	11.7(13)	240.8	20.0(41)	1416.9	41.0(156)	14156.0
10	2	8.0(4)	0.1	10.6(10)	0.3	13.8(15)	0.5	15.1(15)	0.6
	3	8.0(4)	0.7	13.1(12)	3.5	19.3(31)	14.7	24.6(30)	21.5
	4	6.4(5)	6.7	13.5(12)	28.7	20.6(46)	167.6	34.1(67)	449.5
	5	6.6(5)	59.1	12.3(13)	273.1	21.7(58)	2291.8	41.4(162)	15118.4*
10^2	2	4.5(2)	0.1	9.8(6)	0.2	12.3(10)	0.3	15.5(12)	0.5
	3	4.3(2)	0.3	10.3(6)	1.1	15.7(16)	5.2	27.2(24)	18.5
	4	4.6(3)	2.7	9.6(6)	9.7	18.4(20)	61.5	33.2(47)	321.4
	5	5.6(3)	69.3	8.5(7)	196.7	17.6(23)	907.8	34.3(82)	7428.8
10^3	2	3.0(2)	0.1	5.0(3)	0.1	10.1(7)	0.2	13.6(9)	0.3
	3	2.5(2)	0.1	5.0(3)	0.3	10.1(7)	1.4	22.3(12)	6.8
	4	2.5(2)	0.2	4.5(4)	3.7	9.5(7)	12.1	21.1(15)	58.9
	5	3.0(2)	25.9	4.2(4)	66.4	8.2(8)	237.4	19.3(17)	2277.6*

TABLE 6.5

AS-GMRES-IPF *for a variety of values for* $h = 2^{-p}$, ν *and* $\beta = (\beta_1, 0, 0)$. *The symbol '*' denotes runs where an* HSL-MI20 *warning occurred; in some of these cases, much larger timings were observed. Top:* `CC-Pb1`. *Bottom:* `CC-Pb2`.

shows that the number of nonlinear iterations is quite different between AS-GMRES-IPF and AS-MINRES-BDF when h is small and $\nu \in \{10^{-6}, 10^{-8}\}$. For these values the preconditioner in AS-MINRES-BDF is rather ill-conditioned and its performance deteriorates. In this case, the Newton steps computed with the two preconditioned solvers, using the stopping criterion (6.1), might differ so greatly that different convergence histories take place. Unfortunately, this resulted in the AS-MINRES-BDF failure in 10 instances. We recovered 9 over 10 failures by imposing the stricter tolerances $\tau_s = \tau_1 = 10^{-12}$ in (6.1) (this runs are marked with the symbol '†' in Table 6.6). A few unexpected large values of LI can still be observed in Table 6.6 for $\beta = 100$ and $h = 2^{-5}$, which can be presumably ascribed to an inaccuracy of the multigrid operator.

The superiority of AS-GMRES-IPF is also evident in the left plot of Figure 6.1, which reveals that AS-GMRES-IPF is much more efficient than AS-MINRES-BDF in terms of total CPU time and that in the 55% of the runs, the CPU time employed by AS-

	p	$\nu = 10^{-2}$		$\nu = 10^{-4}$		$\nu = 10^{-6}$		$\nu = 10^{-8}$	
β_1		LI(NLI)	TCPU	LI(NLI)	TCPU	LI(NLI)	TCPU	LI(NLI)	TCPU
0	2	20.0(3)	0.2	13.8(7)	0.2	22.7(9)	0.4	25.4(9)	0.4
	3	19.5(4)	4.2	23.8(11)	14.4	34.6(19)	35.8	40.1(27)	57.6
	4	18.7(4)	9.9	23.5(17)	51.6	44.9(54)	289.8	72.1(66)	513.4
	5	19.2(4)	144.4	24.3(15)	474.3	56.3(89)	5627.2	-	-
10	2	18.3(3)	0.1	18.3(10)	0.3	25.3(10)	0.5	29.0(10)	0.5
	3	17.7(4)	4.2	24.6(13)	19.0	37.7(18)	39.7	50.6(19)	56.7
	4	17.7(4)	10.8	26.5(13)	40.0	53.7(33)	245.7	87.7(42)	500.7
	5	19.2(4)	98.4	29.5(15)	550.6	63.1(74)	5572.9	174.1(146)†	$> 5h$*†
10^2	2	10.5(2)	0.1	14.0(4)	0.1	20.5(6)	0.2	31.5(8)	0.4
	3	11.6(3)	1.8	20.2(5)	5.2	27.1(12)	17.4	53.5(19)	54.3
	4	11.6(3)	5.3	20.5(6)	17.8	37.0(14)	72.8	93.5(40)	546.5
	5	98.3(3)	737.3	28.5(6)	382.7	74.8(19)†	2988.0*†	180.2(80)†	$> 5h$*†
10^3	2	6.5(2)	0.1	8.5(2)	0.1	11.5(4)	0.1	17.5(6)	0.2
	3	7.5(2)	0.9	10.5(2)	1.1	11.8(6)	4.0	29.0(8)	13.5
	4	9.5(2)	3.1	13.5(2)	4.3	16.8(6)	15.6	41.1(10)	61.7
	5	9.5(2)	79.4	11.6(3)	146.3	19.0(7)	549.3	42.1(16)	3036.1*

	p	$\nu = 10^{-2}$		$\nu = 10^{-4}$		$\nu = 10^{-6}$		$\nu = 10^{-8}$	
β_1		LI(NLI)	TCPU	LI(NLI)	TCPU	LI(NLI)	TCPU	LI(NLI)	TCPU
0	2	18.0(4)	0.2	23.2(9)	0.4	26.5(12)	0.6	23.1(11)	0.5
	3	16.8(5)	4.7	27.7(13)	19.8	36.8(22)	44.6	35.5(19)	37.1
	4	16.2(5)	11.1	28.7(14)	52.1	43.5(36)	204.8	69.0(63)	572.0
	5	16.6(5)	96.7	27.5(13)	416.1	52.5(53)	3152.0	123(133)†	$> 5h$†
10	2	16.7(4)	0.1	23.0(10)	0.4	32.4(15)	0.9	37.4(15)	1.0
	3	16.5(4)	4.0	30.6(12)	21.7	52.2(30)	90.8	70.3(30)	122.1
	4	14.2(5)	10.8	32.0(12)	54.6	63.7(47)	409.8	108(79)	1151.1
	5	14.8(5)	98.8	33.0(13)	533.3	78.4(100)	$> 5h$	194(159)†	$> 5h$*†
10^2	2	9.5(3)	0.1	20.6(6)	0.2	27.1(10)	0.4	35.6(12)	0.7
	3	9.0(3)	1.5	22.0(6)	7.0	37.3(16)	31.5	66.2(25)	86.9
	4	9.6(3)	4.7	22.1(6)	19.1	47.1(20)	138.3	90.9(56)	744.5
	5	226(3)	1206.2	112.5(7)	1411.8	109.2(23)†	4762.4†	-	-
10^3	2	5.5(2)	0.1	10.3(3)	0.1	21.0(7)	0.3	28.4(9)	0.5
	3	5.5(2)	0.6	10.3(3)	1.8	20.4(7)	7.7	49.6(11)	31.3
	4	5.5(2)	2.3	10.0(4)	6.6	19.5(7)	21.2	63.8(15)†	699.3†
	5	6.5(2)	71.1	8.0(5)	8.3	25.5(8)†	828.3†	67.7(26)†	7897.7†

TABLE 6.6

AS-MINRES-BDF *for a variety of values for* $h = 2^{-p}$, ν *and* $\beta = (\beta_1, 0, 0)$. *The symbol '*' denotes runs where an MI20 warning occurred; in some of these cases, much larger timings were observed (*$> 5h$ *means that the CPU is larger than 5 hours). Top:* `CC-Pb1`. *Bottom:* `CC-Pb2`.

MINRES-BDF is within a factor 2 of the time employed by AS-GMRES-IPF.

Finally, for the sake of completeness, we also carried out experiments on `CC-pb1` using the AGMG algebraic multigrid operator [21, 22] in place of the HSL-MI20 in the solution of systems with L_1. The implementation of AGMG requires the use of the "flexible" variant of the linear system solver since the application of multigrid preconditioner is the result of an iterative process and therefore it changes step by step [28]. Table 6.7 shows the results obtained using Flexible GMRES (FGMRES) in combination with HSL-MI20 (first two columns) and AGMG (last two columns) in the application of the $\mathcal{P}_k^{IPF}$ preconditioner. We only report experiments with $\nu \in \{10^{-6}, 10^{-8}\}$, as for larger values the performance with the two multigrid preconditioners is very similar. For $\nu = 10^{-6}$ the overall performance in terms of CPU time is still somewhat comparable, whereas it is clearly in favor of AGMG in the extreme case $\nu = 10^{-8}$. On the other hand, the average number of iterations (LI) with HSL-MI20 is in general lower, showing that the latter preconditioner is more effective in terms of approximation properties, but more expensive to apply.

		AS-FGMRES-IPF with HSL-MI20				AS-FGMRES-IPF with AGMG			
		$\nu = 10^{-6}$		$\nu = 10^{-8}$		$\nu = 10^{-6}$		$\nu = 10^{-8}$	
β_1	p	LI(NLI)	TCPU	LI(NLI)	TCPU	LI(NLI)	TCPU	LI(NLI)	TCPU
0	2	10.3(9)	0.3	11.1(9)	0.4	17.0(9)	0.3	18.7(9)	0.3
	3	16.0(19)	21.3	18.3(27)	36.4	23.7(19)	12.3	28.5(27)	27.4
	4	17.6(54)	223.6	28.5(57)	351.6	28.5(54)	157.4	41.7(57)	286.7
	5	21.9(68)	2794	38.7(190)	17457.3	44.8(68)	3766.9	53.3(189)	14250
10	2	10.4(10)	0.2	11.3(10)	0.4	19.0(10)	0.2	20.7(10)	0.3
	3	15.4(18)	20.9	19.7(19)	31.1	25.0(18)	11.5	31.7(19)	23.1
	4	18.6(41)	132.6	26.4(42)	239.4	25.0(41)	79.1	35.4(42)	272.3
	5	20.9(47)	1938	37.9(138)	12582*	39.3(47)	1951.3	50.2(147)	10105
10^2	2	10.0(6)	0.1	13.7(8)	0.5	16.0(6)	0.1	20.3(8)	0.3
	3	12.3(12)	10.5	23.7(19)	36.5	20.5(12)	7.5	31.5(19)	24.4
	4	15.1(14)	39.8	36.8(34)	321.0	28.7(14)	37.6	39.4(34)	153.3
	5	14.4(19)	776*	38.8(82)	9172*	39.2(19)	755.6	50.2(81)	5658
10^3	2	6.0(4)	0.1	8.8(6)	0.37	8.2(4)	0.1	12.3(6)	0.2
	3	5.8(6)	2.1	14.1(8)	9.3	9.8(6)	1.2	18.7(8)	5.1
	4	8.1(6)	8.5	20.1(10)	43.2	12.0(6)	5.1	26.3(10)	31.6
	5	7.2(7)	150.1	19.6(16)	1660*	13.1(7)	43.9	26.6(16)	600.6

TABLE 6.7

AS-FGMRES-IPF *(flexible variant) using* HSL-MI20 *(left) and* AGMG *(right) for a variety of values of h and β, and small values of ν. The symbol '*' denotes runs where an* HSL-MI20 *warning occurred; Test problem* `CC-Pb1`.

EXAMPLE 6.3. We further investigate the reliability of our proposals considering problem `CC-pb2` with the following nonconstant convection parameter

$$\beta(x,y,z) = \begin{pmatrix} -2x(1-x)(2y-1)z \\ (2x-1)y(1-y) \\ (2x-1)(2y-1)z(1-z) \end{pmatrix}; \tag{6.2}$$

see example 3D1 in [21]. The performance of AS-GMRES-IPF and AS-MINRES-BDF is analogous to that showed in Tables 6.5-6.6 for the constant and unidirectional $\beta = (\beta_1, 0, 0)$; a sample of this behavior for AS-GMRES-IPF is reported in Table 6.8 as ν and $h - 2^{-p}$ vary.

	AS-GMRES-IPF on `CC-Pb2` with convection (6.2)							
	$\nu = 10^{-2}$		$\nu = 10^{-4}$		$\nu = 10^{-6}$		$\nu = 10^{-8}$	
p	LI(NLI)	TCPU	LI(NLI)	TCPU	LI(NLI)	TCPU	LI(NLI)	TCPU
2	5.0(3)	0.3	9.0(8)	0.4	12.4(19)	0.5	14.5(19)	0.7
3	5.0(3)	2.2	9.4(8)	5.4	15.1(32)	34.2	20.1(41)	66.9
4	4.7(3)	5.9	8.3(9)	14.6	15.4(39)	133.2	26.5(92)	528.8
5	5.0(3)	42.2	7.8(9)	139.9	14.9(36)	1089.0	28.6(137)	9643.7

TABLE 6.8

AS-GMRES-IPF *on problem* `CC-Pb2` *with convection β given in (6.2).*

EXAMPLE 6.4. For the MC and SC problems, we considered $h \in \{2^{-2}, 2^{-3}, 2^{-4}\}$, $\nu \in \{10^{-2}, 10^{-4}, 10^{-6}, 10^{-8}\}$, $\beta = (\beta_1, 0, 0)$ with $\beta_1 \in \{0, 10, 100, 1000\}$, and $\epsilon \in \{10^{-1}, 10^{-2}, 10^{-3}, 10^{-4}, 10^{-8}, 0\}$, where the values $\epsilon \in \{10^{-8}, 0\}$ are included to comprise the SC problems. We thus obtained a set of 288 runs. The numerical results for these problems do not significant differ from those of the CC problem, at least for the larger values of ϵ in the set. Therefore, to avoid proliferation of tables, we prefer not to include them, and report instead the overall performance profile in the right plot of Figure 6.1. For all considered runs, the profile clearly shows that AS-GMRES-IPF

is the fastest in the 96% of the runs and that AS-MINRES-BDF is within a factor 2 of AS-GMRES-IPF for the majority (93%) of the runs.

	$\beta_1 = 10$						$\beta_1 = 100$						
ϵ / ν	-1	-2	-3	-4	-8	$-\infty$	ϵ / ν	-1	-2	-3	-4	-8	$-\infty$
-2	10.3	14.3	35.3	32.5	34.1	34.1	-2	6.0	7.7	8.7	9.0	9.7	9.0
-4	13.5	13.3	16.6	20.2	21.0	21.3	-4	12.3	13.3	16.3	22.3	26.6	26.4
-6	19.5	16.0	14	13.5	13.5	13.5	-6	21.6	19.8	14.7	17.7	16.7	16.7
-8	25.8	18.4	12.0	10.5	10.5	10.5	-8	40.4	34.2	18.0	14.0	13.5	13.5

TABLE 6.9

Mixed Constraints `MC-Pb1`*: Average number of* GMRES *iterations using* AS-GMRES-IPF *with* $h = 2^{-4}$ *and varying* ν *and* ϵ *(*$\log_{10}$ *values of* ν, ϵ*).*

	$\beta_1 = 10$						$\beta_1 = 100$						
ϵ / ν	-1	-2	-3	-4	-8	$-\infty$	ϵ / ν	-1	-2	-3	-4	-8	$-\infty$
-2	22.0	32.1	60.7	86.2	91*	93*	-2	14.0	17.3	19.2	20.0	22.6	21.3
-4	27.8	27.0	34.4	42.2	44.1	44.8	-4	27.0	28.0	33.7	44.2	56.0	55.2
-6	45.3	33.2	27.5	27.5	21.5	27.5	-6	49.4	41.4	29.7	36.0	34.7	34.7
-8	65.7	39.8	24.5	21.5	21.5	21.5	-8	93.6	71.9	36.3	28.5	27.5	27.5

* 6 pre/post smoothing steps set in HSL-MI20

TABLE 6.10

Mixed Constraints `MC-Pb1`*: Average number of* MINRES *iterations using* AS-MINRES-BDF *with* $h = 2^{-4}$ *and varying* ν *and* ϵ *(*$\log_{10}$ *values of* ν, ϵ*).*

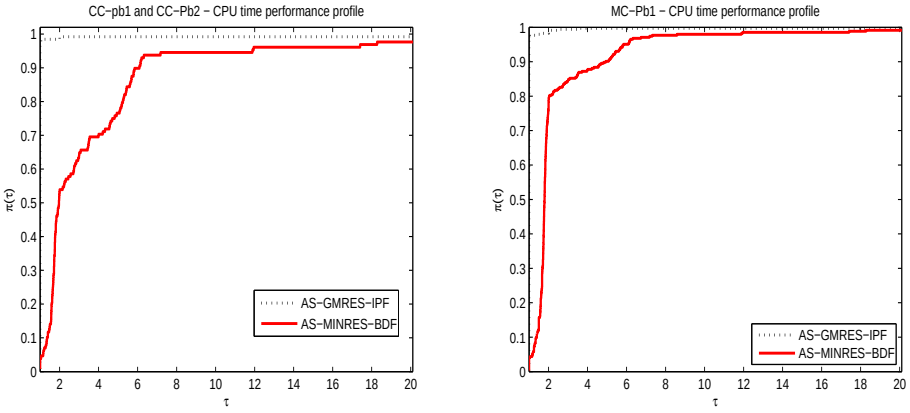

FIG. 6.1. *Total CPU time performance profile for* AS-GMRES-IPF *and* AS-MINRES-BDF. *Left:* `CC-Pb1` *and* `CC-Pb2`. *Right:* `MC-Pb1`.

The dependence on ϵ and the mutual influence of ϵ and ν deserve deeper exploration. In Tables 6.9 and 6.10 we report the average number of inner iterations for $h = 2^{-4}$ obtained with AS-GMRES-IPF and AS-MINRES-BDF, resp., as ν and ϵ vary.

We observe that for $\beta = 10$ the average number of inner iterations becomes large when ϵ is small and ν is large (top right corner) whereas for $\beta = 100$ the increase in iteration number is more evident in the opposite setting (bottom left corner). Overall, the variation of the reported values is quite modest and smallest values are located on the diagonal of the table (shaded cells), i.e. when $\nu = \epsilon^2$. We recall that $\nu = \epsilon^2$ corresponds to $\gamma_1 = \gamma_2 = \frac{1}{2}$ in the block L_1 of the Schur approximation (4.2), so that Proposition 4.7 holds (see Remark 4.8). We also notice that the variation in the

number of iterations is significantly less pronounced for the indefinite preconditioner than for the block diagonal preconditioner. In particular, for a fixed ν, the average number of iterations for AS-GMRES-IPF varies very mildly. More significant variations for fixed ν are visible for AS-MINRES-BDF, see Table 6.10. Moreover, we observe that the behavior of the proposed preconditioner does not deteriorate for $\epsilon \to 0$ and, in particular, fully satisfying results are obtained for $\epsilon = 0$, i.e. in the solution of State Constrained problems.

We point out that similar digits were observed when using a direct solver (not reported here) in place of HSL-MI20 within the preconditioners. Therefore, the different performance as the parameters deviate from $\nu = \epsilon^2$ is not due to the preconditioner inexactness, but rather, to the different quality of the (exact) preconditioner itself. The only exception is given by the two runs marked with the symbol '*' in Table 6.10, for which a lower average number of MINRES iterations was observed when using a direct solver in place of HSL-MI20.

6.2.3. The inexact active-set Newton method for CC problems. Performing the experiments on problems with CC constraints (1.2), we observed different trends in the nonlinear iteration progress varying the parameters ν and β, see e.g. the values of NLI in Table 6.5. To clarify this issue, we plot in Figure 6.2 the convergence history of AS-GMRES-IPF on `CC-Pb1` with mesh size $h = 2^{-4}$ varying $\beta_1 \in \{0, 10, 100, 1000\}$ and setting $\nu = 10^{-2}$ in the left plot and $\nu = 10^{-6}$ in the right plot.

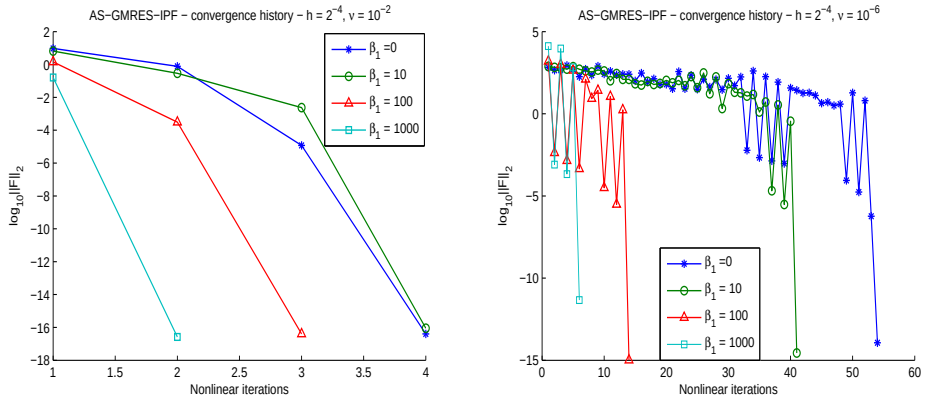

FIG. 6.2. *Convergence history of* AS-GMRES-IPF *for the* `CC-pb1` *with* $h = 2^{-4}$. *Left:* $\nu = 10^{-2}$. *Right:* $\nu = 10^{-6}$.

Looking at each plot we note that the number of nonlinear iterations decreases as β becomes larger; moreover, comparing the two plots, we observe an increase of Newton steps for a smaller ν. More interestingly, the right plot in Figure 6.2 shows a long stagnation phase in the nonlinear process before reaching the local area of fast Newton convergence. In this first phase, away from a solution, choosing an η_k too small (as in (6.1)) can lead to oversolving the Newton equation (2.8): the corresponding step may result in little or no progress toward a solution, while involving pointless expense.

We therefore combined the active-set method with the inexact adaptive choice (2.12). We report in Table 6.11 the results of AS-GMRES-IPF using the adaptive value $\eta_k = \eta_k^I$ in (2.12) on problem `CC-Pb1` with $h \in \{2^{-4}, 2^{-5}\}$, $\beta_1 \in \{0, 10, 100, 1000\}$ and $\nu \in \{10^{-2}, 10^{-4}, 10^{-6}, 10^{-8}\}$.

		$\nu = 10^{-2}$		$\nu = 10^{-4}$		$\nu = 10^{-6}$		$\nu = 10^{-8}$	
β_1	p	LI(NLI)	TCPU	LI(NLI)	TCPU	LI(NLI)	TCPU	LI(NLI)	TCPU
0	4	3.2(5)	3.2	4.5(18)	15.9	7.0(60)	77.1	13.1(131)	281.9
	5	4.0(6)	59.1	2.7(16)	102.0	3.5(92)	646.4	-	-
10	4	3.5(4)	3.2	3.2(14)	11.1	5.2(60)	65.9	112.7(101)	233.9
	5	4.0(5)	39.6	2.9(15)	100.7	3.0(53)	377.7*	-	-
100	4	3.0(3)	1.8	3.3(6)	4.1	11.6(14)	30.4	10.6(51)	100.5
	5	4.3(3)	25.4	3.1(6)	42.1	2.9(27)	332.4*	-	-
1000	4	2.5(2)	1.1	3.3(3)	2.1	7.5(6)	8.5	20.4(10)	45.1
	5	2.5(2)	18.1	3.0(3)	31.6	2.5(7)	67.3	8.1(18)	924.1

TABLE 6.11
AS-GMRES-IPF *on* `CC-Pb1` *for* $h = 2^{-p} \in \{2^{-4}, 2^{-5}\}$ *and a variety of values for* ν *and* β. *The symbol '*' denotes runs where an* HSL-MI20 *warning occurred.*

Let us compare values in Table 6.11 with the corresponding values in Table 6.5 (top table) obtained with η_k^E. The average number of linear iterations is smaller in Table 6.11 than in Table 6.5 while the number of nonlinear iterations is larger in 15 over 29 successful runs. Overall, the saving in number of inner iterations of AS-GMRES-IPF with η_k^I makes it faster than AS-GMRES-IPF with η_k^E in all runs. Two extra failures occur when η_k^I is used in the limit case $\nu = 10^{-8}$.

Summarizing, the inexact strategy is both cheaper and more effective in solving problem (2.4), especially for $\nu \in \{10^{-4}, 10^{-6}\}$ and $\beta_1 \leq 10$, that is values for which the stagnation phase is longer. Note that in particular, a less stringent inner accuracy allows a fast solution also in the limit case $\beta_1 = 1000$.

7. Conclusions. We have proposed two classes of preconditioners (a positive definite one and an indefinite one) for efficiently solving problem (1.1) by means of an active-set Newton method. Both acceleration strategies rely on a new effective approximation to the Schur complement of the Jacobian matrix, for which spectral estimates are provided.

A large set of numerical experiments shows the great potential of these preconditioners for a large range of all problem parameters. As opposed to the current literature, we cope with the indefiniteness of the problem by appropriately choosing the structured preconditioner, and we include active set information explicitly in the preconditioning blocks to exploit this information at later stages. Therefore, the preconditioner adapts dynamically with the modification of the active sets. This procedure allowed us to devise a general and simple to implement acceleration strategy, that can be employed either within MINRES (in the block diagonal form) or within GMRES (in the indefinite factorized form). The latter formulation outperforms MINRES in all test cases, and shows significantly lower sensitivity to the extreme values of the parameters. In general, memory requirements of GMRES remain modest, as the number of iterations stays quite small throughout the nonlinear process. For the smallest values of ν, however, the number of GMRES iterations may make its memory requirements undesirably high. In this case, a short-term recurrence such as the symmetric version of QMR could be considered as an alternative; see, e.g., [26] for a discussion and related numerical experiments. We also mention that a dimension reduction could be employed in the original system (2.8). This strategy is discussed in [32] in the case when no bound constraints are imposed, and it could be naturally generalized to our setting.

Although some of the preconditioner blocks need to be recomputed at each Newton iteration, this cost does not seem to penalize the overall performance of the pre-

conditioned solver. Numerical comparisons with state-of-the-art methods available in the literature support these claims.

Finally, we mention that more general regularization terms could be considered for the cost functionals, for instance, by enforcing sparsity constraints, see, e.g., [33]. We aim to address this important aspect in future research.

Acknowledgements. We would like to thank U. Langer, J. Pearson, M. Stoll, A. Wathen and W. Zulehner for helpful discussions on the topic of this paper. Finally, we aknowledge the insightful remarks of two anonymous referees.

REFERENCES

[1] M. Bergounioux, K. Ito, and K. Kunisch, *Primal-dual strategy for constrained optimal control problems*, SIAM Journal on Control and Optimization, 37 (1999), pp. 1176–1194.
[2] A. Borzì, *Smoothers for control- and state-constrained optimal control problems*, Computing and Visualization in Science, 11 (2007), pp. 59–66.
[3] J. Boyle, M. Mihajlović, and J. Scott, *HSL_MI20: An efficient AMG preconditioner for finite element problems in 3D*, International Journal for Numerical Methods in Engineering, 82 (2010), pp. 64–98.
[4] J. H. Bramble and J.E. Pasciak, *A preconditioning technique for indefinite systems resulting from mixed approximations of elliptic problems*, Mathematics of Computation, 50 (1988), pp. pp. 1–17.
[5] E. Casas, *Control of an elliptic problem with pointwise state constraints*, SIAM Journal on Control and Optimization, 24 (1986), pp. 1309–1318.
[6] F.H. Clarke, *Optimization and Nonsmooth Analysis*, Wiley New York, 1983.
[7] M. D'Apuzzo, V. De Simone, and D. di Serafino, *On mutual impact of numerical linear algebra and large-scale optimization with focus on interior point methods*, Computational Optimization and Applications, 45 (2010), pp. 283–310.
[8] E.D. Dolan and J.J. Moré, *Benchmarking optimization software with performance profiles*, Mathematical Programming, 91 (2002), pp. 201–213.
[9] S. C. Eisenstat and H. F. Walker, *Choosing the forcing term in an inexact Newton method*, SIAM Journal on Scientific Computing, 17 (1996), pp. 16–32.
[10] H.C. Elman, A. Ramage, and D.J. Silvester, *IFISS: A Matlab toolbox for modelling incompressible flow*, ACM Transactions on Mathematical Software, 33 (2007).
[11] H.C. Elman, D.J. Silvester, and A.J. Wathen, *Finite elements and fast iterative solvers: with applications in incompressible fluid dynamics*, Numerical Mathematics and Scientific Computation, Oxford University Press, New York, 2005.
[12] B. Fischer, A. Ramage, D.J. Silvester, and A.J. Wathen, *Minimum residual methods for augmented systems*, BIT, 38 (1998), pp. 527–543.
[13] G. Golub, D. Silvester, and A.J. Wathen, *Diagonal dominance and positive definiteness of upwind approximations for advection diffusion problems*, in Numerical analysis, World Sci. Publ., River Edge, NJ, 1996, pp. 125–131.
[14] R. Herzog and E. Sachs, *Preconditioned Conjugate Gradient method for optimal control problems with control and state constraints*, SIAM Journal on Matrix Analysis and Applications, 31 (2010), pp. 2291–2317.
[15] M. Hintermüller, K. Ito, and K. Kunisch, *The Primal-Dual Active Set strategy as a semismooth Newton method*, SIAM Journal on Optimization, 13 (2002), pp. 865–888.
[16] K. Ito and K. Kunisch, *Semi-smooth Newton methods for state-constrained optimal control problems*, Systems & Control Letters, 50 (2003), pp. 221 – 228.
[17] Ch. Kanzow, *Inexact semismooth Newton methods for large-scale complementarity problems*, Optimization Methods and Software, 19 (2004), pp. 309–325.
[18] K. Kunisch and A. Rösch, *Primal-dual active set strategy for a general class of constrained optimal control problems*, SIAM Journal on Optimization, 13 (2002), pp. 321–334.
[19] The MathWorks, Inc., *MATLAB 7*, R2013b ed., 2013.
[20] Ch. Meyer, U. Prüfert, and F. Tröltzsch, *On two numerical methods for state-constrained elliptic control problems*, Optimization Methods and Software, 22 (2007), pp. 871–899.
[21] Y. Notay, *Aggregation-based algebraic multigrid for convection-diffusion equations*, SIAM Journal on Scientific Computing, 34 (2012), pp. A2288–A2316.
[22] ———, *AGMG software and documentation*, http://homepages.ulb.ac.be/∼ynotay/AGMG, (2014).

[23] J. Pearson, M. Stoll, and A.J. Wathen, *Preconditioners for state constrained optimal control problems with Moreau-Yosida penalty function*, Numerical Linear Algebra with Applications, (2011), pp. 81–97.
[24] J.W. Pearson and A.J. Wathen, *A new approximation of the Schur complement in preconditioners for PDE-constrained optimization*, Numerical Linear Algebra with Applications, 19 (2012), pp. 816–829.
[25] ———, *Fast iterative solvers for convection-diffusion control problems*, Electronic Transactions on Numerical Analysis, 40 (2013), pp. 294–310.
[26] I. Perugia and V. Simoncini, *Block-diagonal and indefinite symmetric preconditioners for mixed finite element formulations*, Numerical Linear Algebra with Applications, 7 (2000), pp. 585–616.
[27] M. Porcelli, *On the convergence of an inexact Gauss-Newton trust-region method for nonlinear least-squares problems with simple bounds*, Optimization Letters, 7 (2013), pp. 447–465.
[28] Y. Saad, *Iterative methods for sparse linear systems*, SIAM, Society for Industrial and Applied Mathematics, 2nd ed., 2003.
[29] Y. Saad and M. H. Schultz, *GMRES: A generalized minimal residual algorithm for solving nonsymmetric linear systems*, SIAM Journal on Scientific and Statistical Computing, 7 (July 1986), pp. 856–869.
[30] J. Schöberl and W. Zulehner, *Symmetric indefinite preconditioners for saddle point problems with applications to PDE-constrained optimization problems*, SIAM Journal on Matrix Analysis and Applications, 29 (2007), pp. 752–773.
[31] D. Sesana and V. Simoncini, *Spectral analysis of inexact constraint preconditioning for symmetric saddle point matrices*, Linear Algebra and its Applications, 438 (2013), pp. 2683–2700.
[32] V. Simoncini, *Reduced order solution of structured linear systems arising in certain PDE-constrained optimization problems*, Computational Optimization and Applications, (2012), pp. 591–617.
[33] G. Stadler, *Elliptic optimal control problems with L1-control cost and applications for the placement of control devices*, Computational Optimization and Applications, 44 (2009), pp. 159–181.
[34] M. Stoll and A.J. Wathen, *Preconditioning for partial differential equation constrained optimization with control constraints*, Numerical Linear Algebra with Applications, (2012), pp. 53–71.
[35] M. Stynes, *Numerical methods for convection-diffusion problems or the 30 years war*, arXiv:1306.5172, Department of Mathematics, National University of Ireland, (2013).
[36] A.J. Wathen and T. Rees, *Chebyshev semi-iteration in preconditioning for problems including the mass matrix.*, ETNA. Electronic Transactions on Numerical Analysis, 34 (2008), pp. 125–135.

Appendix. In this appendix we collect some of the technical proofs (subscript k is omitted).

Proof of Lemma 4.6. From $F + F^T \succeq 0$ it also follows that $F + I$ is nonsingular.

i) We consider the eigenvalue problem $(F+I)^{-1}(F-I)(F-I)^T(F+I)^{-T}x = \theta x$ with $\theta \geq 0$, or, equivalently, $(F - I)(F - I)^T y = \theta(F + I)(F + I)^T y$ with $y = (F + I)^{-T}x$. The largest eigenvalue coincides with $\|(F + I)^{-1}(F - I)\|^2$. We have $(F - I)(F - I)^T = FF^T + I - F - F^T$ and $(F + I)(F + I)^T = FF^T + I + F + F^T$. Substituting and rearranging terms gives

$$(1 - \theta)(FF^T + I)y = (\theta + 1)(F + F^T)y.$$

We multiply from the left by y^T. Since $FF^T + I \succ 0$, $F + F^T \succeq 0$ and $\theta + 1 > 0$, it must be that $1 - \theta \geq 0$, that is $\theta \leq 1$.

ii) We proceed in a similar way. Let us now consider $(F + I)^{-1}(F + F^T)(F + I)^{-T}x = \theta x$, with $\theta > 0$, which is equivalent to $(F + F^T)y = \theta(F + I)(F + I)^T y$, with $y = (F + I)^{-T}x$. Therefore, $(1 - \theta)(F + F^T)y = \theta(FF^T + I)y$. We premultiply by y^T and rearrange to obtain

$$\frac{1 - \theta}{\theta} = \frac{y^T(FF^T + I)y}{y^T(F + F^T)y}.$$

From the relation $(F-I)(F-I)^T \succeq 0$ it follows that $\dfrac{y^T(FF^T+I)y}{y^T(F+F^T)y} \geq 1$. Thus, $\dfrac{1-\theta}{\theta} \geq 1$ which implies $\theta \leq \dfrac{1}{2}$. □

Proof of Proposition 4.9. Let $F = \sqrt{\nu} M^{-\frac{1}{2}} L M^{-\frac{1}{2}}$.

i) For $\alpha_u = 1$ and $\alpha_y = 0$ we have $\gamma_1 = 0$ and $\gamma_2 = 1$, so that $M^{-\frac{1}{2}} \mathbb{S} M^{-\frac{1}{2}} = FF^T + (I - \Pi)$, and

$$M^{-\frac{1}{2}} \widehat{\mathbb{S}} M^{-\frac{1}{2}} = (F + (I-\Pi))(F + (I-\Pi))^T,$$

where we used the fact that $(I-\Pi)^{\frac{1}{2}} = (I-\Pi)$. From $M^{-\frac{1}{2}} \mathbb{S} M^{-\frac{1}{2}} x = \lambda M^{-\frac{1}{2}} \widehat{\mathbb{S}} M^{-\frac{1}{2}} x$ we obtain for $y = M^{\frac{1}{2}} x$

$$(F + (I-\Pi))^{-1}(FF^T + (I-\Pi))(F + (I-\Pi))^{-T} y = \lambda y. \tag{7.1}$$

Since F is nonsingular, we have

$$\begin{aligned}
&(F + (I-\Pi))^{-1}(FF^T + (I-\Pi))(F + (I-\Pi))^{-T} \\
&= (F + (I-\Pi))^{-1} F (I + F^{-1}(I-\Pi)(I-\Pi)F^{-T}) F^T (F + (I-\Pi))^{-T} \\
&= (I + F^{-1}(I-\Pi))^{-1}(I + F^{-1}(I-\Pi)(I-\Pi)F^{-T})(I + F^{-1}(I-\Pi))^{-T} \\
&=: (I+Z)^{-1}(I + ZZ^T)(I+Z)^{-T},
\end{aligned}$$

with $Z = F^{-1}(I-\Pi)$. Therefore, from (7.1) it follows

$$\begin{aligned}
\lambda &\leq \|(I+Z)^{-1}(I+ZZ^T)(I+Z)^{-T}\| \leq \|(I+Z)^{-1}\|^2 + \|(I+Z)^{-1}Z\|^2 \\
&= \|(I+Z)^{-1}\|^2 + \|I - (I+Z)^{-1}\|^2 \\
&\leq \|(I+Z)^{-1}\|^2 + (1 + \|(I+Z)^{-1}\|)^2.
\end{aligned} \tag{7.2}$$

We then recall that $Z = F^{-1}(I-\Pi) = \frac{1}{\sqrt{\nu}} M^{\frac{1}{2}} L^{-1} M^{\frac{1}{2}} (I-\Pi)$, so that

$$\begin{aligned}
\|(I+Z)^{-1}\| &= \|(I + \frac{1}{\sqrt{\nu}} M^{\frac{1}{2}} L^{-1} M^{\frac{1}{2}} (I-\Pi))^{-1}\| \\
&= \|M^{\frac{1}{2}} \left(\sqrt{\nu} L + M(I-\Pi)\right)^{-1} \sqrt{\nu} L M^{-\frac{1}{2}}\|.
\end{aligned}$$

To analyze the behavior for $\nu \to 0$, let us suppose that $L + L^T \succ 0$, and write $Z = \frac{1}{\sqrt{\nu}} \widetilde{F}^{-1}(I-\Pi)$; without loss of generality also assume that $I - \Pi = \mathrm{blkdiag}(I_\ell, 0)$. The eigendecomposition of $\widetilde{F}^{-1}(I-\Pi)$ is given by[4] $\widetilde{F}^{-1}(I-\Pi) = X \Lambda X^{-1}$ where $\Lambda = \mathrm{diag}(\lambda_i)$ and $\lambda_i \in \mathrm{spec}((\widetilde{F}^{-1})_{11}) \cup \{0\}$. Here $(\widetilde{F}^{-1})_{11}$ is the top left $\ell \times \ell$ block of $\widetilde{F}^{-1}$. Note that all eigenvalues of $(\widetilde{F}^{-1})_{11}$ have strictly positive real part, thanks to the condition $L + L^T \succ 0$. Therefore

$$\|(I+Z)^{-1}\| = \|X(I + \frac{1}{\sqrt{\nu}}\Lambda)^{-1} X^{-1}\| \leq \mathrm{cond}(X) \max \left\{ \frac{1}{\min\limits_{\lambda \in \mathrm{spec}((\widetilde{F}^{-1})_{11})} |1 + \lambda/\sqrt{\nu}|}, 1 \right\}.$$

[4] In the unlikely case of a Jordan decomposition, the proof proceeds with the maximum over norms of Jordan blocks inverses, which leads to the same final result.

We thus have

$$\max\left\{\frac{1}{\min\limits_{\lambda\in\mathrm{spec}((\tilde{F}^{-1})_{11})}|1+\lambda/\sqrt{\nu}|},1\right\}\to 1 \qquad \text{for} \qquad \nu\to 0,$$

so that $\|(I+Z)^{-1}\|\le\eta\,\mathrm{cond}(X)$ with $\eta\to 1$ for $\nu\to 0$.

ii) For $\alpha_u=0$ and $\alpha_y=1$ we have $\gamma_1=1$ and $\gamma_2=0$, so that $M^{-\frac{1}{2}}\mathbb{S}M^{-\frac{1}{2}}=F(I-\Pi)F^T+I$, and

$$M^{-\frac{1}{2}}\widehat{\mathbb{S}}M^{-\frac{1}{2}}=(F(I-\Pi)+I)(F(I-\Pi)+I)^T.$$

As before, setting this time $Z=F(I-\Pi)$ we obtain the bounds (7.2) for λ with $\|(I+Z)^{-1}\|=\|(I+\sqrt{\nu}M^{-\frac{1}{2}}LM^{-\frac{1}{2}}(I-\Pi))^{-1}\|$. Finally, it is apparent from the above expression that $\|(I+Z)^{-1}\|\to 1$ as $\nu\to 0$. □